
Seeking Interpretability and Explainability in Binary Activated Neural Networks

Benjamin Leblanc¹ Pascal Germain¹

Abstract

We study the use of binary activated neural networks as interpretable and explainable predictors in the context of regression tasks on tabular data; more specifically, we provide guarantees on their expressiveness, present an approach based on the efficient computation of SHAP values for quantifying the relative importance of the features, hidden neurons and even weights. As the model’s simplicity is instrumental in achieving interpretability, we propose a greedy algorithm for building compact binary activated networks. This approach doesn’t need to fix an architecture for the network in advance: it is built one layer at a time, one neuron at a time, leading to predictors that aren’t needlessly complex for a given task.

1. Introduction

Among machine learning models, decision trees are commonly referred as models of choice on tasks where the interpretability of the predictor is of importance (Xin et al., 2022; Molnar, 2022; Rudin et al., 2021). This contrasts with neural networks (NNs), often perceived as obfuscated black boxes. In this work, we explore the idea that NNs with limited complexity are potentially interpretable models, when constructed with this objective in mind.

Various techniques have been proposed to lighten deep neural networks (DNNs); in addition to being natural regularizer (Hubara et al., 2016; Lin et al., 2019), the use of weights encoded by a small number of bits (Qin et al., 2020; Courbariaux et al., 2015; Meng et al., 2020) and quantized activation functions, notably binary activation functions (Soudry et al., 2014; Hubara et al., 2016; Wang et al., 2019), have shown promising results. Also, methods such as network pruning (Han et al., 2015b; Renda et al., 2020; Hu et al., 2016; Iandola et al., 2016; Goetschalckx et al., 2018), weight sharing (Chen et al., 2015) or matrix factorization (Jaderberg et al., 2014) allow compacting a trained NN, resulting

in predictors having less parameters.

Nevertheless, when one seeks a *light* (interpretable) network, using the aforementioned processes turns out to be tedious as they involve many manipulations: as a first step, large neural network models must be trained (potentially with various combinations of hyperparameters and architectures). Then, these *heavy* networks must be pruned. As implied by the Lottery Ticket Hypothesis from Frankle & Carbin (2019), in order to obtain an efficient compact network from a pruned bigger network, the latter must be big enough so that the chances are high that, within a few different random seeds, it contains a compact but performing sub-network. Working backward would be an interesting avenue for obtaining such networks without needing important computational resources to train wide and deep NNs first; starting with small NNs and making them grow, just like a decision tree is built. Unfortunately, while it’s been shown that greedy approaches can scale to colossal problems such as ImageNet (Belilovsky et al., 2019), the literature concerning greedy approach for training NNs is scarce (Kulkarni & Karande, 2017; Bengio et al., 2006; Dereventsov et al., 2019), and does not exploit the idea that such a method could lead to compact predictors which complexity depends on the task at hand. In this work, we set our sights on neural networks with (simple) binary activation as a model that can be learned greedily and lead to an interpretable predictor on tabular data, similarly as what is usually done with decision trees.

Our contributions are two folds. We first propose a comprehensive study of binary activated networks capabilities for regression tasks, to understand better this particular family of predictors. We introduce a method, based on SHAP values (Lundberg & Lee, 2017), for highlighting the importance of each input features, but also the contribution of hidden neurons and weights of the network in the decision process. We then propose a greedy learning algorithm for building one layer at a time, one neuron at a time a compact fully connected binary activated neural networks for regression tasks. Therefore, the architecture of the resulting predictor is not fixed in advance: it will vary depending on the complexity of the tackled problem. Theoretically well-grounded, this approach uses the fact that a layer’s binary activation can be seen as a hyperplane separating the preceding layer’s output space. The parameters of hidden layers

¹University Laval, Quebec, Canada. Correspondence to: Benjamin Leblanc <benjamin.leblanc.2@ulaval.ca>, Pascal Germain <pascal.germain@ift.ulaval.ca>.

neurons are obtained by computing a Lasso regression on the output of the preceding layer. The obtained predictors are thus compact (because of the greedy approach), sparse (because of the use of Lasso regression), rapidly trainable and efficient in a testing setting (because of the binary activation functions). The algorithm, referred as Binary Greedy Network (BGN) and inspired by Adaboost (Freund & Schapire, 1996), has convergence guarantees on the training mean squared error (MSE). That is, each layer learned by BGN minimizes a lower bound on the MSE obtainable by the global network.

2. Related Works

Interpretability and explainability In line with Rudin (2019), we define the degree of *interpretability* of a predictor by the capacity of a non-expert to understand its decision process solely by considering the model in itself. Therefore, the number of features considered by a neural network, its width, depth and sparseness directly impact its interpretability. This concept greatly differs from *explaining* a model, where explanations present inherently hidden information on the model concerning its decision process. For example, SHAP values (Lundberg & Lee, 2017) explain the impact of the different features of a model on its predictions. The explanations, in machine learning, are usually simplifications of the original model (Fel & Vigouroux, 2020; Subramanian et al., 2018; Ribeiro et al., 2016).

A few families of machine learning models are oftenly considered as possibly interpretable models (Rudin et al., 2021): decision trees, decision lists (rule lists), scoring systems, linear models, etc. Even though effort has been put to explain neural networks, up to the author’s knowledge, they never have been considered as interpretable predictors.

Binary activated neural networks (BANNs) Neural networks learning mostly relies on stochastic gradient descent (SGD), which requires the objective function to be fully differentiable. Because the derivative of a binary function (a function whose output can only take two different values) is zero almost everywhere, this technique cannot directly be used for training with binary activations. Most of the literature concerning BANNs propose workarounds allowing the use of the SGD algorithm. A simple way to estimate the gradient of the binary function is the straight-through estimator (Bengio et al., 2013; Hubara et al., 2016), which uses the identity function as a surrogate of the gradient and which has then been refined over time (Darabi et al., 2018; Liu et al., 2018). While such methods are convenient, they lack solid theoretical groundings. It has also been proposed to use continuous binarization (Gong et al., 2019; Yang et al., 2019; Sakr et al., 2018); continuous activation functions are used, increasingly resembling a binary activation

functions over the training iterations. Another branch of BANNs training algorithms consists of assuming a probability distribution on the weights of the network; doing so, one can work with the expectation of each layers output and train BANNs with the SGD algorithm (Soudry et al., 2014; Letarte et al., 2019).

Greedy neural network training Greedy approaches for training DNNs usually refers to the use of a layer-wise training scheme (Belilovsky et al., 2019; Kulkarni & Karande, 2017; Bengio et al., 2006; Hao et al., 2021; Custode et al., 2020). The usual procedure is the following: first, the full network is trained. Then, the first layer of the network is fixed. The network is retrained, where each layer but the first is fine-tuned. The second layer of the network is then fixed, and so on.

3. Background and Notation

Our study is devoted to univariate and multivariate regression tasks on tabular data. Each task is characterized by a dataset $S = \{(\mathbf{x}_i, \mathbf{y}_i)\}_{i=1}^m$ containing m examples, each one described by features $\mathbf{x} \in \mathcal{X}$ and labels $\mathbf{y} \in \mathbb{R}^d$. From this dataset, we want to train a binary activated neural network (BANN), *i.e.*, with activation functions on hidden layers having two possible output values. Every binary activation function can be described by three parameters $t, h_1, h_2 \in \mathbb{R}$, where $h_1 < h_2$, as follows:

$$f_{t, h_1, h_2}(x) = \begin{cases} h_1 & \text{if } x < t, \\ h_2 & \text{otherwise.} \end{cases} \quad (1)$$

Unless otherwise specified, we use the sign activation function, obtained with $t = 0, h_1 = -1$ and $h_2 = +1$.

We consider fully-connected BANNs composed of $l \in \mathbb{N}^*$ layers L_k of size d_k , for $k \in \{1, \dots, l\}$. We denote d_0 the size of the network input and d_l the size of its output (thus, $d_l = d$). We call l the depth of the network, d_k the width of layer L_k and $d_{\max} = \max_{k \in \{1, 2, \dots, l\}} d_k$ the width of the network. The sequence $\mathbf{d} := \langle d_k \rangle_{k=0}^l$ constitutes the neural network architecture. We denote a BANN predictive function by $B : \mathcal{X} \rightarrow \mathbb{R}^{d_l}$. Every predictor B is characterized by the values of its weights $\{\mathbf{W}_k\}_{k=1}^l$ and biases $\{\mathbf{b}_k\}_{k=1}^l$, where $\mathbf{W}_k \in \mathbb{R}^{d_{k-1} \cdot d_k}$ and $\mathbf{b}_k \in \mathbb{R}^{d_k}$. Each layer L_k is a function

$$L_k(\mathbf{x}) = f_k(\mathbf{W}_k \mathbf{x} + \mathbf{b}_k), \quad (2)$$

where all but the last layers $f_k(\cdot)$ ($k \in \{1, \dots, l-1\}$) are binary activation functions acting element-wise; the output layer $f_l(\cdot)$ being a linear activation (identity) function, allowing predicting real-valued output. For $i, j \in \{1, \dots, l\}$ and $i < j$, we denote

$$L_{i:j}(\mathbf{x}) = (L_j \circ L_{j-1} \circ \dots \circ L_i)(\mathbf{x}).$$

The whole predictor B is given by the composition of all of its layers: $B(\mathbf{x}) = L_{1:l}(\mathbf{x})$ While \mathcal{X} denotes the input space (domain) of the network, $\mathcal{L}_{i:j}$ denotes the image of the function given by the composition of layers L_i to L_j (with $\mathcal{L}_i := \mathcal{L}_{i:i}$) and $\mathcal{B} := \mathcal{L}_{1:l}$ the image of the whole network.

4. Binary Activated Neural Networks: A study

4.1. The binary activation function

We first study the parametrization of the binary activation function of Equation (1). While most previous work on BANNs use of the sign function (Yang et al., 2019; Darabi et al., 2018) or the threshold function (parametrized as follows : $t = 0$, $h_1 = 0$ and $h_2 = 1$) (Letarte et al., 2019; Hubara et al., 2016; Liu et al., 2018), attempts have been made to directly consider h_1 , h_2 and/or t as hyperparameters to optimize (Sakr et al., 2018). We emphasize that the choices of t , h_1 and h_2 doesn't matter, as long as $h_1 \neq h_2$ and that no restrictions are made toward weights and biases values.

Proposition 1. *Let B be a BANN parametrized by $\{\mathbf{W}_k, \mathbf{b}_k\}_{k=1}^l$ such that its activation functions are f_{t,h_1,h_2} . The same goes for B^* , having binary functions f_{t^*,h_1^*,h_2^*} . For all $t, h_1, h_2, t^*, h_1^*, h_2^* \in \mathbb{R}$, there exist weights and biases $\{\mathbf{W}_k^*, \mathbf{b}_k^*\}_{k=1}^l$ parametrizing B^* such that*

(i) B^* has the same architecture as B ;

(ii) $B^*(\mathbf{x}) = B(\mathbf{x}) \forall \mathbf{x} \in \mathbb{R}^{d_0}$;

$$(iii) \mathbf{W}_k^* = \begin{cases} \mathbf{W}_k & \text{if } k = 1, \\ \mathbf{W}_k \begin{matrix} h_1 - h_2 \\ h_1^* - h_2^* \end{matrix} & \text{if } k \in \{2, \dots, l\}, \end{cases}$$

$$\mathbf{b}_k^* = \begin{cases} \mathbf{b}_k + (t^* - t) & \text{if } k = 1, \\ \mathbf{b}_k + (t^* - t) - \mathbf{c}_k & \text{if } k \in \{2, \dots, l-1\}, \\ \mathbf{b}_k - \mathbf{c}_k & \text{if } k = l, \end{cases}$$

$$\text{with } \mathbf{c}_k = \frac{h_1 h_2^* - h_1^* h_2}{h_1^* - h_2^*} \left(\sum_j \mathbf{w}_{k,j} \right).$$

The proof can be found in appendices, section C.1. Let $\mathcal{P}_{\mathbf{d},t,h_1,h_2}$ be the space of neural network predictors obtainable while having architecture \mathbf{d} and binary activation functions f_{t,h_1,h_2} . Proposition 1 informs us that if no restrictions are made toward weights and biases values, then the predictor space $\mathcal{P}_{\mathbf{d},t,h_1,h_2}$ is independent of t , h_1 and h_2 . However, this is not necessarily true if the weights or biases are constrained to specific values, such as binary values (Hubara et al., 2016; Meng et al., 2020), ternary values (Li & Liu, 2016; Zhu et al., 2017; Deng & Zhang, 2020; Hwang & Sung, 2014), low-bit values (Leng et al., 2018; Zhou et al., 2018; Lybrand & Saab, 2021; Krishnamoorthi,

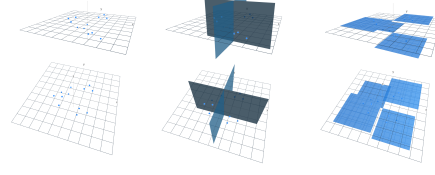


Figure 1. Different layers of a BANN with architecture $\mathbf{d} = \langle 2, 2, 1 \rangle$ acting in its input space \mathcal{X} . Left: x-axis and y-axis represent the feature space of a 2D problem, z-axis being the label space. Middle: the hidden layer of the network separates its input space into regions with $d_1 = 2$ hyperplanes. Right: predictions rendered by the network as a function of its input; the predictions are constant in each region defined by the preceding layer.

2018), etc. In these cases, t , h_1 and h_2 are hyperparameters of the model that needs to be validated.

4.2. A hyperplane arrangement

Each neuron of layers L_1 to L_{l-1} of a BANN can be seen as a hyperplane acting in the input space of the network (L_1) or the output space of the preceding layer (L_2 to L_{l-1}). Indeed, given an input \mathbf{x} , these neurons apply a binary function on a linear function of \mathbf{x} (see Equation (2)). The result indicates whether \mathbf{x} is on one side (h_1) or the other (h_2) of a hyperplane parametrized by the coefficients $\{\mathbf{w}, b\}$ characterizing the neuron. Therefore, a layer composing a BANN is nothing else than a hyperplane arrangement, and the output $f_k(\mathbf{x}) \in \{h_1, h_2\}^{d_k}$ of layer L_k indicates in which region created by the hyperplane arrangement is the input \mathbf{x} . Figure 1 illustrates that phenomenon.

From the observation that the output space of layers L_1 to L_{l-1} is discrete and finite, the following relation can be established for any BANN: $|\mathcal{B}| \leq |\mathcal{L}_{1:l-1}| \leq \dots \leq |\mathcal{L}_1|$. In a few words, this means that the cardinality of the image of the function $(L_k \circ L_{k-1} \circ \dots \circ L_1)(\cdot)$ cannot grow with $k, k < l$. Therefore, when using a BANN predictor, the width of the leading hidden layers shouldn't be neglected, since it has the most impact on the capacity of the network to assign different predictions to different inputs. Thus, a good rule of thumb for selecting the architecture of a fully-connected BANN is to ensure that $d_{l-1} \leq d_{l-2} \leq \dots \leq d_1$.

A network equipped with a too narrow first hidden is able to render only a few unique predictions. As explained above, layer L_{k+1} defines regions in the output space of layer L_k and $|\mathcal{L}_{1:k+1}| \leq |\mathcal{L}_{1:k}|$. Therefore, some of the regions defined by layer L_k are grouped together by layer L_{k+1} . A binary activated neural network can thus be defined the following way: L_1 cuts the input space of a BANN into a set of regions; L_2 to L_{l-1} group several of these regions together; L_l assigns a prediction to each grouped region. This observation leads us to the next proposition, establishing bounds on the training performance of the network in terms of mean

squared error (MSE). Indeed, those bounds are obtained by analyzing every regions independently created by a hidden layer of a BANN.

Proposition 2.1. *Let B be a BANN of depth l . The mean squared error $Q(B, S)$ of predictor B on a dataset S of size m is such that*

$$Q(B, S) := \sum_{(\mathbf{x}, \mathbf{y}) \in S} \frac{\|B(\mathbf{x}) - \mathbf{y}\|^2}{m} \geq g(l-1) \geq \dots \geq g(1),$$

where $\|\cdot\|$ is the Euclidean norm, and

$$g(k) = \sum_{j=1}^{d_k} \sum_{\mathbf{p} \in \mathcal{L}_{1:k}} \frac{|\mathbf{y}_{\mathbf{p},j}^k|}{m} \text{Var}(\mathbf{y}_{\mathbf{p},j}^k), \quad (3)$$

with $\mathbf{y}_{\mathbf{p},j}^{(k)} = \{y_{i,j} \mid (\mathbf{x}_i, \mathbf{y}_i) \in S, (L_k \circ \dots \circ L_1)(\mathbf{x}_i) = \mathbf{p}\}$.

The bound given by Equation (3) can be interpreted as the weighted sum of label's variances associated with the examples grouped in regions created by a layer; the less the points falling the a same region (at any hidden layer in the network) have dissimilar labels, the less is the obtainable mean squared error. Note that a similar bound can be obtained for classification tasks on the 0-1 loss (see appendices, section C.2, along with the proof of Proposition 2.1).

4.3. Expressiveness of BANNs over ReLU networks

Given a regression task, we naturally expect that a BANN needs more parameters than ReLU networks to obtain similar accuracy, but how many more? In order to quantify the expressiveness power of such NNs, we consider the required number of parameters in order to estimate any function from $F_{n,d}$ with an error of at most ϵ . $F_{n,d}$ corresponds to the space of functions from a Sobolev space $\mathcal{W}^{n,\infty}([0,1]^d)$, $n, d \in \mathbb{N}^*$, having a norm upper bounded by 1. This metric is borrowed from previous works studying the expressiveness power of several NN architectures, from ReLU networks (Yarotsky, 2017; 2018; Perekrestenko et al., 2018) to networks with quantized weights (Ding et al., 2019), and even networks having both ReLU and binary activation functions (Ding et al., 2019; Liang & Srikant, 2017), but never BANNs. For more details on Sobolev functional spaces, see appendices, section A.7.

Inspired by the work of Yarotsky (2017), we provide in Theorem 1 lower and upper bounds on that required number of parameters (see section C.3 and section C.4 for proofs).

Theorem 1. *For $n, d \in \mathbb{N}^*$, there exists a binary activated network capable of estimating any function from $F_{n,d}$ with maximum absolute error ϵ for which:*

(i) the width of the first hidden layer (and of the global network) is in $O(c\epsilon^{-(d/n+1)})$, where c is a constant depending on n and d ,

(ii) the depth is constant, depending on n and d ,

(iii) the number of weights is in $\Omega(c\epsilon^{-d/n} \ln^{-1}(\epsilon^{-1}))$.

Notice that in Theorem 1, since the depth is constant, then the upper bound from (i) also holds for the number of weights. Equations (4-7) below summarize lower and upper bounds for BANNs as well as those holding for ReLU networks, which are taken from Yarotsky (2017).

$$\Omega \text{ ReLU} : c\epsilon^{-(d/2n)} \quad (4)$$

$$\Omega \text{ BANN} : c\epsilon^{-d/n} \ln^{-1}(\epsilon^{-1}) \quad (5)$$

$$O \text{ ReLU} : c\epsilon^{-d/n} \ln(\epsilon^{-1}) \quad (6)$$

$$O \text{ BANN} : c\epsilon^{-(d/n+1)} \quad (7)$$

Notice that the ratio O/Ω for BANNs is $\epsilon^{-1} \ln(\epsilon^{-1})$, which depends solely on ϵ ; the ratio O/Ω for ReLU networks is $\epsilon^{-(d/2n)} \ln(\epsilon^{-1})$, therefore relying additionally on d and n . Hence, the tightness of the bounds does not depend on the input dimension for BANNs while it matters for ReLU networks. Since using a large n is restrictive, because $|F_{n+1,d}| \leq |F_{n,d}| \forall n, d \in \mathbb{N}^*$, and that the input dimension d is potentially large when it comes to function estimation problems, then the bounds might just be tighter for BANNs than ReLU networks for several function estimation problems. Notice that the ratio ‘‘O Binary over O ReLU’’ is $\epsilon^{-1} / \ln(\epsilon^{-1})$, which increases less than linearly with ϵ^{-1} . As such, the number of weights needed for a BANN in order to obtain the same performance as a ReLU network a given tasks might not be as important as intuitively expected, even when the required maximum absolute error is truly small.

5. SHAP values for BANNs

SHAP values (Lundberg & Lee, 2017) is a metric quantifying the impact (magnitude) of the feature values on the predictions of a given model. They are widely used due to their simplicity and theoretical grounding. The main drawback of the SHAP values is their computational cost, which is exponential regarding the number of features of the model. An algorithm named TreeSHAP (Lundberg et al., 2018) has been designed in order to efficiently compute the SHAP values for tree ensemble predictors; with t being the number of trees in the ensemble, s the maximum number of leaves per tree, l is the maximum depth of a tree, m the number of examples in the training dataset and d_0 the number of features, SHAP values originally had a computational cost in $O(m \cdot t \cdot s \cdot 2^{d_0})$. By exploiting the structure of decision trees, TreeSHAP has a complexity of $O(m \cdot t \cdot s \cdot l^2)$. It is a significant computational gain, since 2^{d_0} can be intractable and l^2 is generally small.

5.1. Efficiently computing the SHAP values of a BANN

We use the fact that a single hidden layer BANN (denoted 1-BANN below) can be seen as an aggregation of hyperplane predictors, whose SHAP values can be computed independently in order to efficiently compute the SHAP values of those shallow BANNs for regression purposes. The proposed algorithm, denoted 1-BANN SHAP in the following, computes SHAP values of a binary activated neural network in $O(m^2 \cdot d_0 \cdot d_{\max} \cdot 2^n)$, where d_{\max} is the network width and n is the maximum number of non-zero weights a neuron of the first hidden layer has.

Note that Algorithm 1 does not directly return SHAP values, but a $d \times d \times |L_1|$ tensor \mathbf{R} , which values that require to be aggregated in a way such that the resulting vector of length d contains SHAP values associated with the input features. Forthcoming Section 5.2 explains how \mathbf{R} can be analyzed in different ways to compute complementary information.

Algorithm 1 1-BANN SHAP

```

1: Input :  $\{\mathbf{x}_1, \dots, \mathbf{x}_m\}$ ,  $\mathbf{x} \in \mathbb{R}^d$ , the features of dataset
2:        $B$ , a BANN;  $\{\mathbf{W}_1, \dots, \mathbf{W}_l\}$ , its weights
3:  $\mathbf{R} = \mathbf{0}_{d \times d \times |L_1|}$ 
4:  $\mathbf{C} = \mathbf{0}_{1 \times d}$ 
5: For  $g \in \{1, \dots, |L_1|\}$  :
6:    $\mathbf{a} = \mathbb{1}_{\{\mathbf{w}_g \neq 0\}}$ 
7:    $\mathbf{C} = \mathbf{C} \cup \text{comb}(\mathbf{a})$ 
8: For  $i \in \{1, \dots, d\}$  such that  $(\exists j \mid c_{j,i} = 1)$ :
9:   For  $j \in \{1, \dots, |\mathbf{C}|\}$  such that  $c_{j,i} = 1$  :
10:    For  $\mathbf{x}, \mathbf{x}' \in S$  :
11:     If  $L_1(\mathbf{x}_{\mathbf{c} \setminus \{j\}} \cup \mathbf{x}'_{\mathbf{c} \setminus \{j\}}) \neq L_1(\mathbf{x}_{\mathbf{c}} \cup \mathbf{x}'_{\mathbf{c}})$  :
12:       $\mathbf{r}_{i,|c_{j,i}|_1} = \mathbf{r}_{i,|c_{j,i}|_1} + \frac{\theta_{\mathbf{x},f}}{m} \odot \left| \sum_{k=1}^{d_i} \mathbf{w}_k \right|$ ,
13: with  $\theta_{\mathbf{x},f} = \left| L_1(\mathbf{x}_{\mathbf{c} \setminus \{j\}} \cup \mathbf{x}'_{\mathbf{c} \setminus \{j\}}) - L_1(\mathbf{x}_{\mathbf{c}} \cup \mathbf{x}'_{\mathbf{c}}) \right|$ 
14: Return  $\mathbf{R}$ 
    
```

Since each hidden neuron is treated independently, the algorithm is not combinatorial in the number of considered features, but in the maximum number of non-zero weights connecting the input layer to a hidden neuron. The function $\text{comb}(\cdot)$ (Algorithm 1, line 7) computes every combination of features having non-zero weights for each hidden neuron. Further details and generalization of the algorithm to deep architecture are provided in appendices (section A.5).

5.2. SHAP values for hidden neurons and weights

We present two complementary ways of exploiting the tensor \mathbf{R} returned by Algorithm 1. First, aggregating \mathbf{R} values into a vector of length $|L_1|$ gives values that reflect the relative importance of the different hidden neurons in the predictions. Second, aggregating \mathbf{R} values into a $d \times |L_1|$

matrix result in values that reflect the feature relative importance to determine the activation value of individual hidden neurons. This original approach gives information regarding the importance of both the hidden neurons and their respective features. We illustrate experimentally that these information could enhance the explainability of a BANN model in section 7, and we refer the reader to the appendices for the mathematical details allowing performing the tensor values aggregation (section A.5).

6. The Binary Greedy Network (BGN) Algorithm

From the study of binary activated neural networks of section 4, and particularly the observations made in section 4.2, we design an algorithm for greedily building such predictors. We leverage the bounds obtained from Proposition 2.1 as an objective function for parameterizing the hidden layers of the BANNs. We first explain the core algorithm principle in the simple cases of single-hidden layers neural networks and univariate regression tasks. Then, we extend the algorithm to deep and sparse BANNs and multivariate regression tasks.

6.1. BGN algorithm for single-hidden layer neural networks on univariate regression tasks

Consider a single-hidden layer BANN (that is, $l = 2$) with a real-valued input space ($\mathbf{x} \in \mathbb{R}^{d_0}$) and an univariate output ($y \in \mathbb{R}^{d_2}$, with $d_2 = 1$). In order to learn a compact BANN architecture, the proposed BGN algorithm iteratively construct the hidden layer by adding one neuron at the time. Thus, we start by building a network with architecture $\mathbf{d}^{(1)} = \langle d_0, 1, d_2 \rangle$, then adding a neuron on the hidden layer in order to obtain an architecture $\mathbf{d}^{(2)} = \langle d_0, 2, d_2 \rangle$ and so on. Recall that in a BANN, every neuron of a hidden layer can be seen as a hyperplane. The idea is to iteratively minimize the bound from Proposition 2.1 as the layer is built, so that the final predictor has the lowest lower bound on the obtainable MSE. Using the notation defined in Proposition 2.1, we aim to parameterize the first neuron of the hidden layer as follows:

$$\operatorname{argmin}_{\mathbf{w}, b} \left(\frac{|\mathbf{y}_{-1}|}{m} \operatorname{Var}(\mathbf{y}_{-1}) + \frac{|\mathbf{y}_{+1}|}{m} \operatorname{Var}(\mathbf{y}_{+1}) \right), \quad (8)$$

with $\mathbf{y}_{\pm 1} = \{y_j \mid (\mathbf{x}_j, y_j) \in S, \operatorname{sgn}(\mathbf{w} \cdot \mathbf{x}_j + b) = \pm 1\}$. The parameterization neurons to be added subsequently to the hidden layer will aim to minimize that same quantity, but with modified labels. Therefore, we aim to place a hyperplane in the input space such that the weighted sum of the variance of examples falling on each of its side is minimized. Since it is not a convex problem, we rely on a heuristic, which is based on the fact that the hyperplane seeks to separate the points with "large" labels values from points

Algorithm 2 Binary Greedy Network (BGN) - One hidden layer predictor

- 1: **Input** : $S = \{(\mathbf{x}_1, y_1), \dots, (\mathbf{x}_m, y_m)\}$, $y \in \mathbb{R}$, $\mathbf{x} \in \mathbb{R}^d$, a dataset
- 2: T , a number of iteration
- 3: Heuristic(\cdot), a method for placing hyperplanes
- 4: Set $\mathbf{r}^{(1)} = \mathbf{y} = (y_1, \dots, y_m)$
- 5: **For** $t = 1, \dots, T$:
- 6: $\mathbf{w}_t, b_t = \text{Heuristic}(S^{(t)})$, where $S^{(t)} = \{(\mathbf{x}_1, r_1^{(t)}), \dots, (\mathbf{x}_m, r_m^{(t)})\}$
- 7: $c_t, d_t = \frac{1}{2}(\rho_+^{(t)} - \rho_-^{(t)}), \frac{1}{2}(\rho_+^{(t)} + \rho_-^{(t)})$,
with $\rho_{\pm}^{(t)} = \frac{\sum_{i: \text{sgn}(\mathbf{x}_i \cdot \mathbf{w}_t + b_t) = \pm 1} r_i^{(t)}}{\sum_{i: \text{sgn}(\mathbf{x}_i \cdot \mathbf{w}_t + b_t) = \pm 1} 1}$
- 8: $r_i^{(t+1)} = r_i^{(t)} - c_t \text{sgn}(\mathbf{w}_t \cdot \mathbf{x}_i + b_t) - d_t \quad \forall i \in \{1, \dots, m\}$
- 9: **Output** : $BGN_T(\mathbf{x}) = \sum_{t=1}^T c_t \text{sgn}(\mathbf{w}_t \cdot \mathbf{x} + b_t) + d_t$

with "small" labels values. Note that the heuristic uses an auxiliary linear learning algorithm to find the weights of the added neurons, which is reminiscent of the Boosting algorithms that add a predictor to the learned ensemble at every iteration (Freund & Schapire, 1996).

Heuristic 1. Use a Lasso regression (Tibshirani, 1996) algorithm to obtain a weight vector \mathbf{w} (do not consider the obtained bias value). Once \mathbf{w} is fixed, find b minimizing Equation (8).

Note that, in Heuristic 1, finding b minimizing Equation (8) can be computed in $O(m \ln m)$ operations. It is done by sorting the examples by their distance to the hyperplane parametrized by \mathbf{w} , without bias, and computing the obtained MSE on the $m + 1$ possible separation of the sorted dataset. Once the hyperplane is fixed, that is, when parameters $(\mathbf{w}_{1,t}, b_{1,t})$ of the network are fixed, the way parameter $w_{2,t}$ is obtained and b_2 is updated is presented in Proposition 3, where c_t corresponds to $w_{2,t}$ and d_t corresponds to the update on b_2 during iteration t . Algorithm 2 illustrates and summarizes the process of building the single-hidden layer BANN.

Proposition 3. In Algorithm 2, we have

$$(c_t, d_t) = \underset{c, d}{\text{argmin}} \sum_i \left(y_i^{(t)} - c \text{sgn}(\mathbf{w}_t \cdot \mathbf{x}_i + b_t) - d \right)^2.$$

The following proposition informs us that the objective we chose for our hyperplanes to minimize not only optimize the minimum obtainable MSE of the global network, but ensure that at every iteration of the algorithm, *i.e.*, every time a neuron is added to the network, the MSE obtained by the network on its training dataset diminishes.

Proposition 4. In Algorithm 2, $\forall t \in \mathbb{N} \setminus \{0, 1\}$, we have

$$Q(BGN_{t-1}, S) - Q(BGN_t, S) = (c_t + d_t)(c_t - d_t) > 0.$$

6.2. Generalizing the BGN algorithm to sparse and deep predictors and multivariate tasks

A key motivation of our work is to find the model with the right complexity for the task at hand. To enforce the *compactness* and the *sparsity* of the learned BNN, the following two improvements are proposed to the basic BGN algorithm (Algorithm 2).¹

Improvement 1. In order to tackle the drawbacks of the greedy building of a layer, at iteration $t > 1$, the oldest hyperplane that has been placed in the input space (*i.e.*, a hidden neuron) is removed before applying another iteration of the algorithm. Then, if the training error diminishes, the replaced hyperplane (neuron) is kept. Otherwise, the former is placed back. This is done r times.

Improvement 2. To tackle multivariate regression problems where the output is in \mathbb{R}^d , we consider an example $(\mathbf{x}_i, \mathbf{y}_i) = (\mathbf{x}_i, (y_{i,1}, \dots, y_{i,d}))$ as d examples with a single output value when placing the hyperplanes (neurons). That is, we use the Heuristic of Algorithm 2–Line 2 with

$$S^{(t)} = \bigcup_{i=1}^m \{(\mathbf{x}_i, r_{i,j}^{(t)})\}_{j=1}^d,$$

with the residuals initialized to $r_{i,j}^{(1)} = y_{i,j}$ and updated coordinate-wise at Line 2. See the appendices (section A.6) for the whole algorithmic procedure, in which c_t and d_t are also replaced by vectors of dimension d to produce a multivariate output.

Note that the result from Proposition 4 also holds in the multivariate case, but the MSE now diminishes of $(\mathbf{c}_t + \mathbf{d}_t)(\mathbf{c}_t - \mathbf{d}_t)$ at iteration t . Finally, the last improvement allows extending our BGN algorithm to more than one hidden layer.

Improvement 3. A deep BANN is constructed by building the first layer until the MSE on a validation set does not improve more than a chosen criterion; then, a second hidden layer is built using the same technique, but uses the output of the first hidden layer for features of its training dataset; and so on.

7. Numerical Experiments

We conduct two sets of experiments (all of them being performed on 2 NVIDIA GPUs GeForce RTX 2080 Ti). The first one aims to test whether BGN can compete with other techniques from the literature for training BANNs in terms of predictive performance on different regression tasks. The second one aims to verify whether BGN yields

¹The full algorithms implementing the improvements presented in this section are given in the appendices, section A.6.

predictors at least as interpretable as regression trees for similar accuracy.

7.1. Performance experiments

Baselines The first benchmark we compare BGN to is a BANN trained by SGD, with the help of the straight-through estimator (BNN*). We also compare to BNN+ (Darabi et al., 2018), which was inspired by Binarized Neural Network (Hubara et al., 2016) but make use of a refined version of the straight-through estimator. The next two benchmarks use different continuous binarization tricks: Quantization Networks (QN) (Yang et al., 2019) and Bi-real net* (Liu et al., 2018) (adapted to fully-connected architectures). Note that test performances for continuous binarization algorithms are calculated with the use of binary activation functions. We finally present the results obtain by BinaryConnect (Courbariaux et al., 2015), as often seen in the BANN training algorithm’s literature. For each benchmark, three learning rates are tested (0.1, 0.01, 0.001), three different width (100, 500 and 1000 neurons) and depth (1, 2 and 3 hidden layers). For the BNN+ algorithm, L_1 or L_2 regularization are tested, with coefficients 10^{-6} and 10^{-7} . Both QN and BNN+ have a specific hyperparameter (respectively T_{Start} and β), for which three different values were tested (respectively 5, 10, 20 and 1, 2, 5). The Adam (Kingma & Ba, 2015) optimization algorithm is used for every benchmark, along with Kaiming uniform initialization (He et al., 2015). The maximum number of epoch is set to 200.

BGN We evaluate BGN algorithm with Improvements 1, 2 and 3. We used the following procedure for selecting the regularization parameter of the Lasso regression, as we seek a network as sparse as possible: the parameter is set to 10^5 ; while the Lasso regression leads to a solution with all coefficients being 0s (except for the bias), the regularization parameter is divided by 1.5. Parameters r and q (patience) (Improvements 1 and 3) are set to 10 and 20.

Datasets We chose a variety of datasets having different number of examples (315 to 36 736) and input and output cardinality (4 to 20 and 1 to 6). There are 4 different multivariate tasks and 7 univariate tasks. The architecture and hyperparameter set yielding the best average validation MSE over 3 random initialization and train / validation separation are selected, and we report in Table 1 the corresponding architecture and mean test MSE. See the appendices for specific values and more details on the experiment setting, as well as extended details on the considered datasets (section A.1 and section A.2).

7.2. Interpretability and explainability of 1-BANNs

We trained a regression tree of depth three on the *housing* dataset (where the goal is to predict the cost of a house);

$$B(\text{MedInc}, \text{MedAge}, \text{TotalBed}) = 1.00 + 1.27 \cdot \mathbb{1}_{\{\text{MedInc} > 65.46\}} + 1.01 \cdot \mathbb{1}_{\{0.59 \cdot \text{MedAge} + \text{MedInc} > 63.56\}} + 0.60 \cdot \mathbb{1}_{\{\text{MedInc} > 28.20\}} + 0.36 \cdot \mathbb{1}_{\{\text{TotalBed} > 622.0\}} + 0.27 \cdot \mathbb{1}_{\{\text{MedAge} > 20.0\}}$$

Figure 2. A 1-BANN predictor trained on the *housing* dataset. All possible impact on the final prediction, as a function of the features, are explicit.

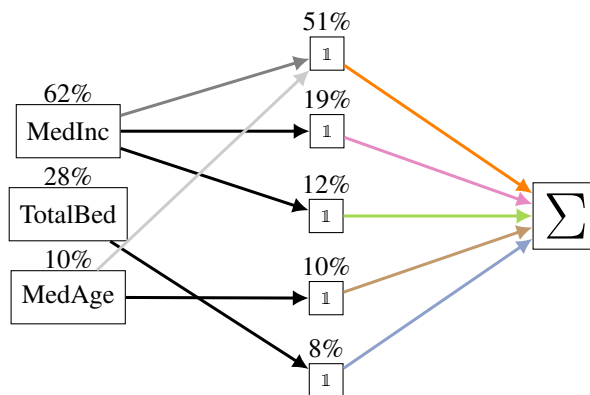


Figure 3. Visual representation of a 1-BANN for the *housing* dataset. The values over the input neurons and hidden neurons correspond to their respective SHAP values, at a predictor level. The blackness of the weights connecting the input layer to the hidden layer is proportional to the SHAP value, at a neuron level.

we then used BGN for growing a 1-BANN until the latter had better performances than the former. Knowing that the depth-3 regression tree is quite interpretable, we now analyse the obtained 1-BANN predictor to see if this one also has interesting interpretability and explainability properties. More details on the hyperparameter tuning of the models can be found in appendices (section A.4).

We present the 1-BANN predictor in two different ways, the first one putting the emphasis on its interpretable aspect (Figure 2), the second one on its explainable aspect (Figure 3). The predictor is presented with threshold activation function for interpretability’s sake. The dataset contains eight features, but only three were retained by the BGN predictor: the median age of a house within a block (MedAge); the total number of bedrooms within a block (TotalBed); the median income for households within a block of houses (measured in thousands of US Dollars) (MedInc).

7.3. Discussion

The performance experiments reported in Table 1 clearly show that BGN is competitive on various regression tasks when compared to several algorithms from the literature for training BANNs. This includes both univariate and multi-

Table 1. Experiment results over 3 repetitions for selected models: MSE obtained on test dataset (Error_T) of the selected predictor, width (l) and depth (d). Lowest MSE per dataset are bolded.

Dataset	BGN			BC			BNN*			BNN+			Bi-real net*			QN		
	Error_T	l	d	Error_T	l	d	Error_T	l	d	Error_T	l	d	Error_T	l	d	Error_T	l	d
bike hour (Fanaee-T & Gama, 2013)	3573.67	259	2	21881.79	1000	3	1948.73	1000	3	1712.45	1000	2	1818.36	1000	3	2008.47	1000	2
carbon (Aci & Avci, 2016)	0.0048	40	1	5.45	100	2	0.82	500	1	0.95	100	1	1.28	1000	1	0.94	500	3
diabete (Efron et al., 2004)	3755.93	6	1	9134.43	500	1	8919.54	1000	1	8999.32	500	2	8816.83	100	1	8811.23	500	2
housing (Harrison & Rubinfeld, 1978)	0.32	158	1	1.65	100	2	2.19	500	1	2.09	1000	1	2.36	500	1	2.16	500	1
hung pox (Rozemberczki et al., 2021)	223.76	3	1	235.75	100	2	250.07	100	2	229.83	100	3	242.55	100	3	214.27	500	3
ist stock usd (Akbilgic et al., 2014)	2.27	5	1	22787.86	100	1	2.98	1000	3	1.95	1000	1	2.42	1000	2	1.94	1000	1
parking (Stolfi et al., 2017)	6954.87	1000	1	176286.81	1000	1	32705.94	500	3	11684.12	1000	3	16543.25	1000	2	107347.98	1000	2
power plant (Tüfekci, 2014; HeysemKaya et al., 2012)	17.18	187	2	13527.9	500	2	18.34	1000	1	16.66	1000	2	16.77	1000	2	17.14	1000	2
solar flare (Dua & Graff, 2017)	0.66	13	1	1.11	1000	3	0.8	100	3	0.71	100	2	0.82	100	3	0.73	100	1
stock portfolio (Liu & Yeh, 2017)	0.0660	32	1	13.58	100	3	3.78	100	1	119.32	1000	3	2.55	100	1	0.36	500	3
turbine (Kaya et al., 2019)	27.91	361	2	3477.78	100	2	21.92	500	3	19.02	1000	2	21.8	500	3	25.54	1000	2

variate regression tasks, as well as small and big datasets, datasets with a few features per example, etc. On some datasets, all of the baseline methods surprisingly fail to provide a good predictor, despite all of the hyperparameter combination that were tested (BGN was used without the need for testing a set of hyperparameters, while the benchmarks had between 27 and 324 hyperparameters combinations to test per dataset). The most surprising result occurs on the *diabete* dataset, where BGN’s MSE is more than two times smaller than the best runner-up. This might be due to the fact that usual neural networks experiments does not focus on regression tasks on tabular data.

Table 1 also highlights that the predictors given by BGN are consistently shallower and narrower than those selected by the baselines. On simple tasks, BGN achieves competitive prediction using very few parameters, whereas the baselines provide predictors containing up to a million parameters. Obtaining, from the baselines, a compact but efficient predictor is not as easy as training a huge one and then pruning it (see the pruning experiments in appendices, section A.3).

As for the interpretability and explainability experiments, Figure 2 presents the equation describing the 1-BANN predictor. The way the neurons (thresholds, in the equation) are independent makes it easier to understand their individual impact (when being active or not) on the final prediction, especially when compared to a regression tree (Figure 6 and Figure 7, section A.4). Both the base prediction (here, 1.00) and each possible way to make this prediction bigger or smaller are explicit because of the additive form of the predictor; this does not stand for decision trees. The 1-BANN can be presented such that only positive values (shown in ascending order) can be added to the base prediction, making the decomposition of the final prediction easier to decompose. Each threshold makes at most two features interact, so that they all remain simple.

Figure 3 presents a visual depiction of the network predictor. Three types of SHAP values are present: two at the predictor level (feature values, above the features; hidden neuron

values, above the hidden neurons), and one at a neuron level (the color intensity of a weight is proportional to its neuron-wise SHAP value). For example, for the only hidden neuron being connected to two features, we see that *MedInc* is more important than *TotalBed*, from the SHAP point of view. The different ways to aggregate the SHAP values present informations that cannot be computed, for example, for tree predictors. Because of the color code linking both representations, it is possible to associate the neurons from Figure 3 to their corresponding equations from Figure 2. Thus, not only do we know the importance of the features, but also of the different hidden neurons and their respective features with BANNs. We argue that this could contribute to explain the model behavior to a non machine learning expert.

8. Conclusion

We provided a comprehensive study of binary activated neural networks (BANNs) in the context of regression tasks; we presented lower and upper bounds on the expressiveness of these particular networks and an algorithm for efficiently computing SHAP values for shallow BANNs, not only for its features, but also for its hidden neurons and their respective features. Using the observations that were made, we designed a greedy algorithm for building compact and sparse BANNs that is theoretically well-grounded. The approach avoid the classical stochastic gradient descent scheme to build the predictor one neuron at a time, one layer at a time, without the need for fixing in advance an architecture. The proposed method also has a training loss-decrease guarantee over each iteration.

We showed that the method is able to tackle both small and big regression problems, obtaining MSE comparable to state-of-the art methods for training BANNs. We presented an analysis of a BANN trained on the *housing* dataset, arguing that the predictor had both interpretability and explainability advantages over a similarly-performing regression tree.

References

- Aci, M. and Avci, M. Artificial neural network approach for atomic coordinate prediction of carbon nanotubes. *Applied Physics A*, 122, 06 2016.
- Akbulgic, O., Bozdogan, H., and Balaban, M. E. A novel hybrid rbf neural networks model as a forecaster. *Statistics and Computing*, 24:365–375, 2014.
- Belilovsky, E., Eickenberg, M., and Oyallon, E. Greedy layerwise learning can scale to imagenet. In *ICML*, volume 97 of *Proceedings of Machine Learning Research*, pp. 583–593. PMLR, 2019.
- Bengio, Y., Lamblin, P., Popovici, D., and Larochelle, H. Greedy layer-wise training of deep networks. In *NIPS*, pp. 153–160. MIT Press, 2006.
- Bengio, Y., Léonard, N., and Courville, A. C. Estimating or propagating gradients through stochastic neurons for conditional computation. *CoRR*, abs/1308.3432, 2013.
- Blalock, D. W., Ortiz, J. J. G., Frankle, J., and Gutttag, J. V. What is the state of neural network pruning? In *MLSys*. mlsys.org, 2020.
- Chen, W., Wilson, J. T., Tyree, S., Weinberger, K. Q., and Chen, Y. Compressing neural networks with the hashing trick. In *ICML*, volume 37 of *JMLR Workshop and Conference Proceedings*, pp. 2285–2294. JMLR.org, 2015.
- Courbariaux, M., Bengio, Y., and David, J. Binaryconnect: Training deep neural networks with binary weights during propagations. In *NIPS*, pp. 3123–3131, 2015.
- Cowan, N. The magical mystery four: How is working memory capacity limited, and why? *Current directions in psychological science*, 19:51–57, 02 2010. doi: 10.1177/0963721409359277.
- Custode, L. L., Tecce, C. L., Bakurov, I., Castelli, M., Cioppa, A. D., and Vanneschi, L. A greedy iterative layered framework for training feed forward neural networks. In *EvoApplications*, volume 12104 of *Lecture Notes in Computer Science*, pp. 513–529. Springer, 2020.
- Darabi, S., Belbahri, M., Courbariaux, M., and Nia, V. P. BNN+: improved binary network training. *CoRR*, abs/1812.11800, 2018.
- Deng, X. and Zhang, Z. An embarrassingly simple approach to training ternary weight networks. *CoRR*, abs/2011.00580, 2020.
- Dereventsov, A., Petrosyan, A., and Webster, C. G. Greedy shallow networks: A new approach for constructing and training neural networks. *CoRR*, abs/1905.10409, 2019.
- Ding, Y., Liu, J., Xiong, J., and Shi, Y. On the universal approximability and complexity bounds of quantized relu neural networks. In *ICLR (Poster)*. OpenReview.net, 2019.
- Dua, D. and Graff, C. UCI machine learning repository, 2017. URL <http://archive.ics.uci.edu/ml>.
- Efron, B., Hastie, T., Johnstone, I., and Tibshirani, R. Least angle regression. *The Annals of statistics*, 32(2):407–499, 2004.
- Fanaee-T, H. and Gama, J. Event labeling combining ensemble detectors and background knowledge. *Progress in Artificial Intelligence*, pp. 1–15, 2013. ISSN 2192-6352.
- Fel, T. and Vigouroux, D. Representativity and consistency measures for deep neural network explanations. *CoRR*, abs/2009.04521, 2020.
- Frankle, J. and Carbin, M. The lottery ticket hypothesis: Finding sparse, trainable neural networks. In *ICLR*. OpenReview.net, 2019.
- Frankle, J., Dziugaite, G. K., Roy, D. M., and Carbin, M. The lottery ticket hypothesis at scale. *CoRR*, abs/1903.01611, 2019.
- Freund, Y. and Schapire, R. E. Experiments with a new boosting algorithm. In *ICML*, pp. 148–156. Morgan Kaufmann, 1996.
- Gale, T., Elsen, E., and Hooker, S. The state of sparsity in deep neural networks. *CoRR*, abs/1902.09574, 2019.
- Goetschalckx, K., Moons, B., Wambacq, P., and Verhelst, M. Efficiently combining svd, pruning, clustering and retraining for enhanced neural network compression. In *EMDL@MobiSys*, pp. 1–6. ACM, 2018.
- Gong, R., Liu, X., Jiang, S., Li, T., Hu, P., Lin, J., Yu, F., and Yan, J. Differentiable soft quantization: Bridging full-precision and low-bit neural networks. In *ICCV*, pp. 4851–4860. IEEE, 2019.
- Han, S., Pool, J., Tran, J., and Dally, W. J. Learning both weights and connections for efficient neural network. In *NIPS*, pp. 1135–1143, 2015a.
- Han, S., Pool, J., Tran, J., and Dally, W. J. Learning both weights and connections for efficient neural networks. *CoRR*, abs/1506.02626, 2015b.
- Han, S., Mao, H., and Dally, W. J. Deep compression: Compressing deep neural network with pruning, trained quantization and Huffman coding. In *ICLR*, 2016.
- Hao, W., Jin, X., Siegel, J. W., and Xu, J. An efficient greedy training algorithm for neural networks and applications in pdes. *CoRR*, abs/2107.04466, 2021.

- Harrison, D. and Rubinfeld, D. L. Hedonic housing prices and the demand for clean air. *Journal of Environmental Economics and Management*, 5(1):81–102, 1978. ISSN 0095-0696.
- He, K., Zhang, X., Ren, S., and Sun, J. Delving deep into rectifiers: Surpassing human-level performance on imagenet classification. In *ICCV*, pp. 1026–1034. IEEE Computer Society, 2015.
- HeysemKaya, T., Tüfekçi, P., and andFikret S. Gürgen. Local and global learning methods for predicting power of a combined gas & steam, 2012.
- Hu, H., Peng, R., Tai, Y., and Tang, C. Network trimming: A data-driven neuron pruning approach towards efficient deep architectures. *CoRR*, abs/1607.03250, 2016.
- Hubara, I., Courbariaux, M., Soudry, D., El-Yaniv, R., and Bengio, Y. Binarized neural networks. In *NIPS*, pp. 4107–4115, 2016.
- Hwang, K. and Sung, W. Fixed-point feedforward deep neural network design using weights +1, 0, and -1. In *SiPS*, pp. 174–179. IEEE, 2014.
- Iandola, F. N., Moskewicz, M. W., Ashraf, K., Han, S., Dally, W. J., and Keutzer, K. Squeezenet: Alexnet-level accuracy with 50x fewer parameters and <1mb model size. *CoRR*, abs/1602.07360, 2016.
- Jaderberg, M., Vedaldi, A., and Zisserman, A. Speeding up convolutional neural networks with low rank expansions. In *BMVC*. BMVA Press, 2014.
- Kaya, H., Tufekci, P., and Uzun, E. Predicting co and nox emissions from gas turbines: novel data and abenchmark pems. *TURKISH JOURNAL OF ELECTRICAL ENGINEERING & COMPUTER SCIENCES*, 27:4783–4796, 11 2019.
- Kingma, D. P. and Ba, J. Adam: A method for stochastic optimization. In *ICLR (Poster)*, 2015.
- Krishnamoorthi, R. Quantizing deep convolutional networks for efficient inference: A whitepaper. *CoRR*, abs/1806.08342, 2018.
- Kulkarni, M. and Karande, S. S. Layer-wise training of deep networks using kernel similarity. *CoRR*, abs/1703.07115, 2017.
- Leng, C., Dou, Z., Li, H., Zhu, S., and Jin, R. Extremely low bit neural network: Squeeze the last bit out with ADMM. In *AAAI*, pp. 3466–3473. AAAI Press, 2018.
- Letarte, G., Germain, P., Guedj, B., and Laviolette, F. Dichotomize and generalize: Pac-bayesian binary activated deep neural networks. In *NeurIPS*, pp. 6869–6879, 2019.
- Li, F. and Liu, B. Ternary weight networks. *CoRR*, abs/1605.04711, 2016.
- Liang, S. and Srikant, R. Why deep neural networks for function approximation? In *ICLR (Poster)*. OpenReview.net, 2017.
- Lin, J., Gan, C., and Han, S. Defensive quantization: When efficiency meets robustness. *CoRR*, abs/1904.08444, 2019. URL <http://arxiv.org/abs/1904.08444>.
- Liu, Y.-c. and Yeh, I.-C. Using mixture design and neural networks to build stock selection decision support systems. *Neural Computing and Applications*, 28, 03 2017.
- Liu, Z., Wu, B., Luo, W., Yang, X., Liu, W., and Cheng, K. Bi-real net: Enhancing the performance of 1-bit cnns with improved representational capability and advanced training algorithm. *CoRR*, abs/1808.00278, 2018.
- Lundberg, S. M. and Lee, S. A unified approach to interpreting model predictions. In *NIPS*, pp. 4765–4774, 2017.
- Lundberg, S. M., Erion, G. G., and Lee, S. Consistent individualized feature attribution for tree ensembles. *CoRR*, abs/1802.03888, 2018.
- Lybrand, E. and Saab, R. A greedy algorithm for quantizing neural networks. *J. Mach. Learn. Res.*, 22:156:1–156:38, 2021.
- Meng, X., Bachmann, R., and Khan, M. E. Training binary neural networks using the bayesian learning rule. In *ICML*, volume 119 of *Proceedings of Machine Learning Research*, pp. 6852–6861. PMLR, 2020.
- Miller, G. A. The magical number seven plus or minus two: some limits on our capacity for processing information. *Psychological review*, 63 2:81–97, 1956.
- Molnar, C. Interpretable machine learning, 2022. URL <https://christophm.github.io/interpretable-ml-book>.
- Perekrestenko, D., Grohs, P., Elbrächter, D., and Bölcskei, H. The universal approximation power of finite-width deep relu networks. *CoRR*, abs/1806.01528, 2018.
- Qin, H., Gong, R., Liu, X., Bai, X., Song, J., and Sebe, N. Binary neural networks: A survey. *Pattern Recognit.*, 105:107281, 2020.
- Renda, A., Frankle, J., and Carbin, M. Comparing rewinding and fine-tuning in neural network pruning. In *ICLR*. OpenReview.net, 2020.

- Ribeiro, M. T., Singh, S., and Guestrin, C. "why should I trust you?": Explaining the predictions of any classifier. In *KDD*, pp. 1135–1144. ACM, 2016.
- Rozemberczki, B., Scherer, P., Kiss, O., Sarkar, R., and Ferenci, T. Chickenpox cases in hungary: a benchmark dataset for spatiotemporal signal processing with graph neural networks, 2021.
- Rudin, C. Stop explaining black box machine learning models for high stakes decisions and use interpretable models instead. *Nat. Mach. Intell.*, 1(5):206–215, 2019.
- Rudin, C., Chen, C., Chen, Z., Huang, H., Semenova, L., and Zhong, C. Interpretable machine learning: Fundamental principles and 10 grand challenges. *CoRR*, abs/2103.11251, 2021.
- Sakr, C., Choi, J., Wang, Z., Gopalakrishnan, K., and Shanbhag, N. R. True gradient-based training of deep binary activated neural networks via continuous binarization. In *ICASSP*, pp. 2346–2350. IEEE, 2018.
- Soudry, D., Hubara, I., and Meir, R. Expectation back-propagation: Parameter-free training of multilayer neural networks with continuous or discrete weights. In *NIPS*, pp. 963–971, 2014.
- Stolfi, D. H., Alba, E., and Yao, X. Predicting car park occupancy rates in smart cities. In Alba, E., Chicano, F., and Luque, G. (eds.), *Smart Cities*, pp. 107–117, Cham, 2017. Springer International Publishing. ISBN 978-3-319-59513-9.
- Subramanian, A., Pruthi, D., Jhamtani, H., Berg-Kirkpatrick, T., and Hovy, E. H. SPINE: sparse interpretable neural embeddings. In *AAAI*, pp. 4921–4928. AAAI Press, 2018.
- Tibshirani, R. Regression shrinkage and selection via the lasso. *Journal of the Royal Statistical Society (Series B)*, 58:267–288, 1996.
- Tüfekci, P. Prediction of full load electrical power output of a base load operated combined cycle power plant using machine learning methods. *International Journal of Electrical Power & Energy Systems*, 60:126–140, 2014. ISSN 0142-0615.
- Wang, Z., Lu, J., Tao, C., Zhou, J., and Tian, Q. Learning channel-wise interactions for binary convolutional neural networks. In *CVPR*, pp. 568–577. Computer Vision Foundation / IEEE, 2019.
- Xin, R., Zhong, C., Chen, Z., Takagi, T., Seltzer, M. I., and Rudin, C. Exploring the whole rashomon set of sparse decision trees. *CoRR*, abs/2209.08040, 2022.
- Yang, J., Shen, X., Xing, J., Tian, X., Li, H., Deng, B., Huang, J., and Hua, X. Quantization networks. *CoRR*, abs/1911.09464, 2019.
- Yarotsky, D. Error bounds for approximations with deep relu networks. *Neural Networks*, 94:103–114, 2017.
- Yarotsky, D. Optimal approximation of continuous functions by very deep relu networks. In *COLT*, volume 75 of *Proceedings of Machine Learning Research*, pp. 639–649. PMLR, 2018.
- Zhou, A., Yao, A., Wang, K., and Chen, Y. Explicit loss-error-aware quantization for low-bit deep neural networks. In *CVPR*, pp. 9426–9435. Computer Vision Foundation / IEEE Computer Society, 2018.
- Zhu, C., Han, S., Mao, H., and Dally, W. J. Trained ternary quantization. In *ICLR (Poster)*. OpenReview.net, 2017.

Appendix

A. Supplementary material

A.1. Extended details on the datasets

Table 2. Datasets overview (C = Categorical, F = Floats, I = Integers)

#	Dataset	Full name	Taken from	Source	y	x	Type of x	Nb. ex.
1	bike hour	Bike sharing dataset	UCI Repo.	(Fanaee-T & Gama, 2013)	1	16	F/I	17 389
2	carbon	Carbon nanotubes	UCI Repo.	(Aci & Avci, 2016)	3	5	F	10 721
3	diabete	Diabetes	SKLearn	(Efron et al., 2004)	1	10	F/I	442
4	housing	California housing	SKLearn	(Harrison & Rubinfeld, 1978)	1	8	F	20 640
5	hung pox	Hungarian chickenpox cases	UCI Repo.	(Rozemberczki et al., 2021)	1	20	F	521
6	ist stock usd	Istanbul stock exchange (USD)	UCI Repo.	(Akbulgic et al., 2014)	1	8	F	536
7	parking	Parking Birmingham	UCI Repo.	(Stolfi et al., 2017)	1	4	F	35 717
8	power plant	Combined cycle power plant	UCI Repo.	(Tüfekci, 2014; HeysemKaya et al., 2012)	1	4	F	9568
9	solar flare	Solar flare	UCI Repo.	(Dua & Graff, 2017)	3	10	C	1389
10	stock portfolio	Stock portfolio performance	UCI Repo.	(Liu & Yeh, 2017)	6	6	F	315
11	turbine	Gas Turbine CO and NOx emission data set	UCI Repo.	(Kaya et al., 2019)	2	10	F	36 733

A.2. Extended details on the performance experiments

Tested hyperparameters

- # Hidden layers : 1,2,3
- Width : 100, 500, 1000
- Learning rates : 0.1, 0.01, 0.001
- Regularization type (BNN+) : L_1 , L_2
- Regularization values (BNN+) : 10^{-6} , 10^{-7}
- β values (BNN+) : 1, 2, 5
- T_{Start} values (QN) : 5, 10, 20 (while $T_{\text{At epoch } n} = T_{\text{Start}} * n$)

Fixed hyperparameters

- Initialization : Kaiming uniform (He et al., 2015)
- Batch size : 512 for big datasets (over 9000 examples) and 64 for small datasets; see Table 2
- Maximum number of epochs : 200
- Loss function : Mean squared error (MSE)
- Optimization algorithm : Adam (Kingma & Ba, 2015)
 - $\epsilon = 0.001$
 - $\rho_1 = 0.9, \rho_2 = 0.999$

Seeking Interpretability and Explainability in Binary Activated Neural Networks

– $\delta = 1e - 8$

– $\lambda = 0$

- Learning rate decay : plateau
- Patience : 5
- Early stop : 20

The test set was always composed of 25% of the total dataset (if the train-test separation isn't inerant to the problem), while the validation set was 20% of the remaining data.

Table 3. Experiment results over 3 repetitions for selected models: mean MSE obtained on test dataset for the selected predictor with standard deviation.

Dataset	BGN	BC	BNN*	BNN+	Bi-real net*	QN
bike hour	3573.67	21881.79	1948.73	1712.45	1818.36	2008.47
	±	±	±	±	±	±
	208.64	6954.39	134.03	144.65	137.1	120.36
carbon	0.0048	5.45	0.82	0.95	1.28	0.94
	±	±	±	±	±	±
	0.0002	2.84	0.32	0.52	0.54	0.08
diabete	3755.93	9134.43	8919.54	8999.32	8816.83	8811.23
	±	±	±	±	±	±
	178.15	432.55	941.61	918.98	1102.82	721.51
housing	0.32	1.65	2.19	2.09	2.36	2.16
	±	±	±	±	±	±
	0.02	0.01	0.19	0.1	0.19	0.13
hung pox	223.76	235.75	250.07	229.83	242.55	214.27
	±	±	±	±	±	±
	14.82	28.42	44.63	34.45	106.58	9.87
ist stock usd	2.27	22787.86	2.98	1.95	2.42	1.94
	±	±	±	±	±	±
	0.06	26955.24	0.63	0.13	0.12	0.08
parking	6954.87	176286.81	32705.94	11684.12	16543.25	107347.98
	±	±	±	±	±	±
	2108.30	863.17	5146.44	2849.72	2690.26	10455.96
power plant	17.18	13527.9	18.34	16.66	16.77	17.14
	±	±	±	±	±	±
	0.42	13271.0	1.0	1.3	1.34	0.67
solar flare	0.66	1.11	0.8	0.71	0.82	0.73
	±	±	±	±	±	±
	0.01	0.38	0.13	0.07	0.12	0.11
stock portfolio	0.0660	13.58	3.78	119.32	2.55	0.36
	±	±	±	±	±	±
	0.0332	8.41	0.57	205.89	0.28	0.2
turbine	27.91	3477.78	21.92	19.02	21.8	25.54
	±	±	±	±	±	±
	2.09	2841.67	1.01	1.34	0.66	0.68

Seeking Interpretability and Explainability in Binary Activated Neural Networks

Table 4. Hyperparameters of selected models over 3 repetitions.

Dataset	Algorithm	Width	Depth	lr	reg. type	λ	T_{start}	β
bike hour	BC	1000	3	0.1	—	—	—	—
	BNN*	1000	3	0.1	—	—	—	—
	BNN+	1000	2	0.1	L2	1e-07	—	2
	Bi-real net*	1000	3	0.1	—	—	—	—
	QN	1000	2	0.01	—	—	5	—
carbon	BC	100	2	0.1	—	—	—	—
	BNN*	500	1	0.1	—	—	—	—
	BNN+	100	1	0.1	L1	1e-07	—	5
	Bi-real net*	1000	1	0.1	—	—	—	—
	QN	500	3	0.01	—	—	5	—
diabete	BC	500	1	0.1	—	—	—	—
	BNN*	1000	1	0.1	—	—	—	—
	BNN+	500	2	0.1	L1	1e-06	—	5
	Bi-real net*	100	1	0.1	—	—	—	—
	QN	500	2	0.1	—	—	5	—
housing	BC	100	2	0.1	—	—	—	—
	BNN*	500	1	0.01	—	—	—	—
	BNN+	1000	1	0.01	L1	1e-06	—	2
	Bi-real net*	500	1	0.01	—	—	—	—
	QN	500	1	0.01	—	—	10	—
hung pox	BC	100	2	0.1	—	—	—	—
	BNN*	100	2	0.1	—	—	—	—
	BNN+	100	3	0.1	L1	1e-07	—	5
	Bi-real net*	100	3	0.1	—	—	—	—
	QN	500	3	0.1	—	—	5	—
ist stock usd	BC	100	1	0.1	—	—	—	—
	BNN*	1000	3	0.001	—	—	—	—
	BNN+	1000	1	0.1	L2	1e-07	—	1
	Bi-real net*	1000	2	0.001	—	—	—	—
	QN	1000	1	0.1	—	—	10	—
parking	BC	1000	1	0.001	—	—	—	—
	BNN*	500	3	0.01	—	—	—	—
	BNN+	1000	3	0.01	L2	1e-06	—	2
	Bi-real net*	1000	2	0.01	—	—	—	—
	QN	1000	2	0.01	—	—	5	—
power plant	BC	500	2	0.1	—	—	—	—
	BNN*	1000	1	0.1	—	—	—	—
	BNN+	1000	2	0.1	L2	1e-06	—	5
	Bi-real net*	1000	2	0.1	—	—	—	—
	QN	1000	2	0.01	—	—	5	—
solar flare	BC	1000	3	0.1	—	—	—	—
	BNN*	100	3	0.1	—	—	—	—
	BNN+	100	2	0.1	L1	1e-07	—	5
	Bi-real net*	100	3	0.01	—	—	—	—
	QN	100	1	0.1	—	—	5	—
stock portfolio	BC	100	3	0.1	—	—	—	—
	BNN*	100	1	0.1	—	—	—	—
	BNN+	1000	3	0.01	L2	1e-06	—	1
	Bi-real net*	100	1	0.1	—	—	—	—
	QN	500	3	0.01	—	—	10	—
turbine	BC	100	2	0.1	—	—	—	—
	BNN*	500	3	0.1	—	—	—	—
	BNN+	1000	2	0.1	L1	1e-07	—	2
	Bi-real net*	500	3	0.1	—	—	—	—
	QN	1000	2	0.01	—	—	5	—

Table 5. Benchmarks overview

Algorithm	BGN	BC	BNN*	BNN+	Bi-real net*	QN
Weights	\mathbb{R}	$\{-1, +1\}$	\mathbb{R}	\mathbb{R}	\mathbb{R}	\mathbb{R}
Activations output	$\{-1, +1\}$	\mathbb{R}	$\{-1, +1\}$	$\{0, 1\}$	$\{-1, +1\}$	$\{0, 1\}$
Uses batch norm*	False	True	True	True	True	True
Uses regularization	False	False	False	True	False	False

*For every algorithm making use of batch normalization, each activation layer is preceded by a batch norm layer. The intrinsic parameters of batch norm layers aren't considered in section A.3.

A.3. Pruning experiments

Procedure We chose two datasets from section 7.1 to test the ability of the considered algorithms to yield compact predictors : Istanbul Stock USD and Power Plant (two datasets where BGN is outperformed by a benchmark). We then took the benchmark algorithm that resulted in the best performances over three different random seed in both of these tasks (respectively BNN+ and QN), with the corresponding set of hyperparameters, and alternately prune the trained network by a factor 0.5 and fine-tune it until only a few parameters were left active (non-zero). The fine-tuning is done by applying the same algorithm as for training, but the learning rate is divided by 10 and the maximum number of epoch is divided by 2. We then compared the reported mean test loss (on 5 different random seeds) over the pruning operation to the test loss BGN obtained while building its predictor. The number of active weights is a common metric for comparing pruning methods (Blalock et al., 2020).

Pruning methods We chose five pruning methods that have been shown to be competitive with more elaborate and complex methods (Frankle et al., 2019; Gale et al., 2019; Han et al., 2015a; 2016) : Global Magnitude Pruning (GMP), Layerwise Magnitude Pruning (LMP), Global Gradient Magnitude Pruning (GGMP), Layerwise Gradient Magnitude Pruning (LGMP). Respectively, at each iteration of the methods, the pruned weights are those with the lowest absolute : value anywhere in the network; value for each layer; value \times associated gradient, evaluated on a batch of inputs, anywhere in the network; value \times associated gradient, for each layer. We also included Random Pruning (each weight is pruned with fixed probability), which is a common straw man in pruning experiments. Since QN uses a continuous binarization trick, the gradient-based pruning methods aren't applicable here.

Table 1 highlights that the predictors given by BGN are consistently shallower and narrower than those selected by the baselines. On simple tasks, BGN achieves competitive prediction using very few parameters, whereas the baselines provide predictors containing up to a million parameters. Obtaining, from the baselines, a compact but efficient predictor is not as easy as training a huge one and then pruning it. Figure 4 and Figure 5 both are inline with that assertion: on both a big (Figure 4) and a small (Figure 5) dataset, pruning the best predictor obtained from a baseline until it contains as few active parameters as the predictor given by BGN truly impact the obtained test MSE. A few pruning methods were tested, but even then, it seems that the best pruning method depends on the problem or the fine-tuning algorithm. When the size of the predictor is not a considered factor, baselines and BGN seems to be truly comparable, but when the predictors are forced to be considerably small, BGN definitely shines.

Tested hyperparameters

- # Hidden layers : 1,2,3
- Width : 100, 500, 1000
- Learning rates : 0.1, 0.01, 0.001
- Regularization type (BNN+) : L_1 , L_2
- Regularization values (BNN+) : 10^{-6} , 10^{-7}
- β values (BNN+) : 1, 2, 5
- T_{Start} values (QN) : 5, 10, 20 (while $T_{\text{At epoch } n} = T_{\text{Start}} * n$)

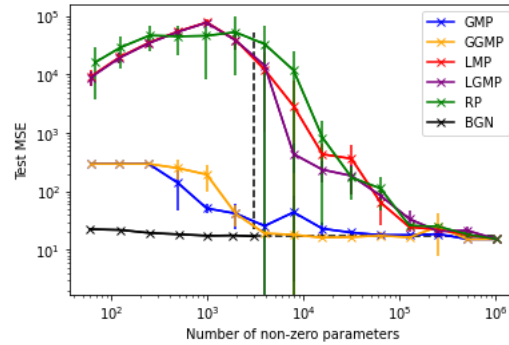


Figure 4. Pruning experiments on the Power Plant dataset with standard deviation over 5 random seeds. Dotted lines show where BGN has converged.

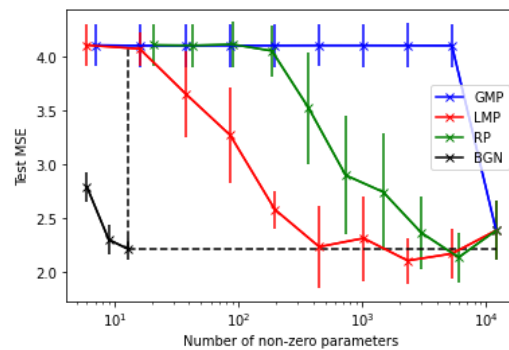


Figure 5. Pruning experiments on the Istanbul Stock USD dataset with standard deviation over 5 random seeds. Dotted lines show where BGN has converged.

A.4. Extended details on the interpretability and explainability experiments

The experiments were conducted on five random seeds, for BGN as well as for the regression tree. As for the tree, the following hyperparameter choices were considered (with the retained set of hyperparameter being bolded): maximum number of features (n) considered at each split: \mathbf{n} , \sqrt{n} , $\log_2(n)$; criterion: **squared error**, friedman mse, absolute error, poisson; the strategy used to choose the split at each node: random, **best**.

Here is a list of different features of the *housing* dataset; recall that the target of this dataset corresponds to the median house value for households within a block (measured in hundreds of thousands of US Dollars):

- Long: A measure of how far west a house is; a higher value is farther west;
- Lat: A measure of how far north a house is; a higher value is farther north;
- MedAge: Median age of a house within a block; a lower number is a newer building;
- totRooms: Total number of rooms within a block;
- totBed: Total number of bedrooms within a block;
- pop: Total number of people residing within a block;
- house: Total number of households, a group of people residing within a home unit, for a block;
- medInc: Median income for households within a block of houses (measured in thousands of US Dollars).

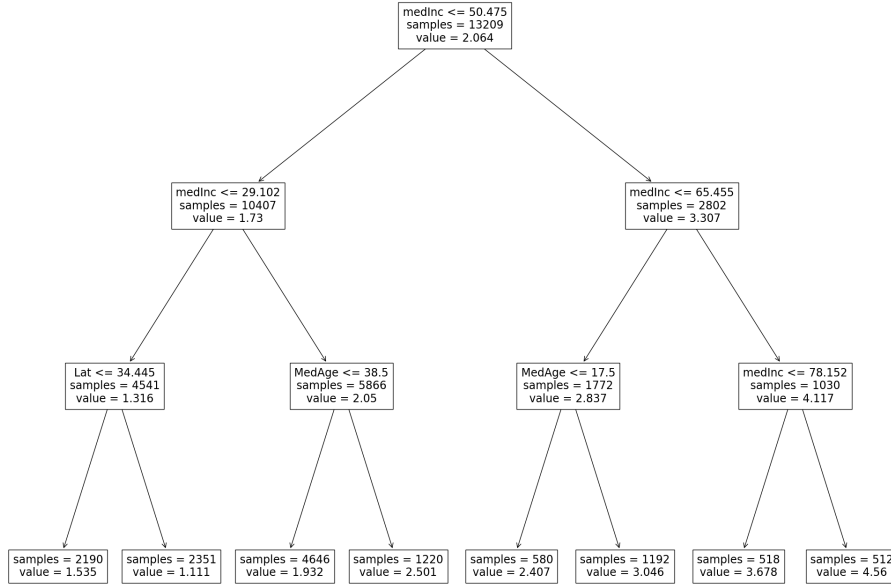


Figure 6. A visual representation of a regression tree of depth three trained on the *housing* dataset.

It seems that, at least in some cases, BGN is able to present more compact and interpretable predictors, for given thresholds of performances, than the regression tree predictor. Figure 6 and Figure 7 respectively present complete regression trees trained on the *housing* dataset and having depths of three and four. If it is ambiguous whether or not the tree of depth three is interpretable, the tree of depth four is clearly too complex for a non expert to understand the decision process of the predictor. In comparison, the corresponding 1-BANN remains quite interpretable, considering that humans can handle at most 7 ± 2 cognitive entities at once (Miller, 1956; Cowan, 2010). Table 6 enforces this idea by comparing trees of depth 3-4-5 to corresponding 1-BANNs obtaining similar validation performances. We see that the width of the 1-BANNs grows almost linearly, for small networks, with the depth of the regression tree for fixed performances; while the depth of the tree has a huge impact on its interpretability, the width of the 1-BANN has a relationship to its interpretability that is way less important.

Figure 8 shows the relationship between a regression trees performances on the *housing dataset* and its depth; the same relationship is depicted for a 1-BANN, but as a function of its width. Because BGN makes a 1-BANN grow in a way that is similar to the growing of a regression tree, than the growth can be stopped whenever the desired compromise performances / simplicity is obtained.

A.5. BANN SHAP Algorithms

Let us first recall what the computation of a single SHAP value (for a single feature and a single example) looks like:

$$\phi_i(f, \mathbf{x}) = \sum_{\underbrace{S \subseteq F \setminus \{i\}}_{(1)}} \underbrace{\frac{|S|!(|F| - |S| - 1)!}{|F|!}}_{(2)} \left(\mathbb{E}_{X_{S \cup \{i\}}} [f(\mathbf{x}_F)] - \mathbb{E}_{X_{\bar{S}}} [f(\mathbf{x}_F)] \right), \quad (9)$$

The function $comb(\cdot)$ (Algorithm 1, line 7) returns an array of the different combination of all positive inputs:

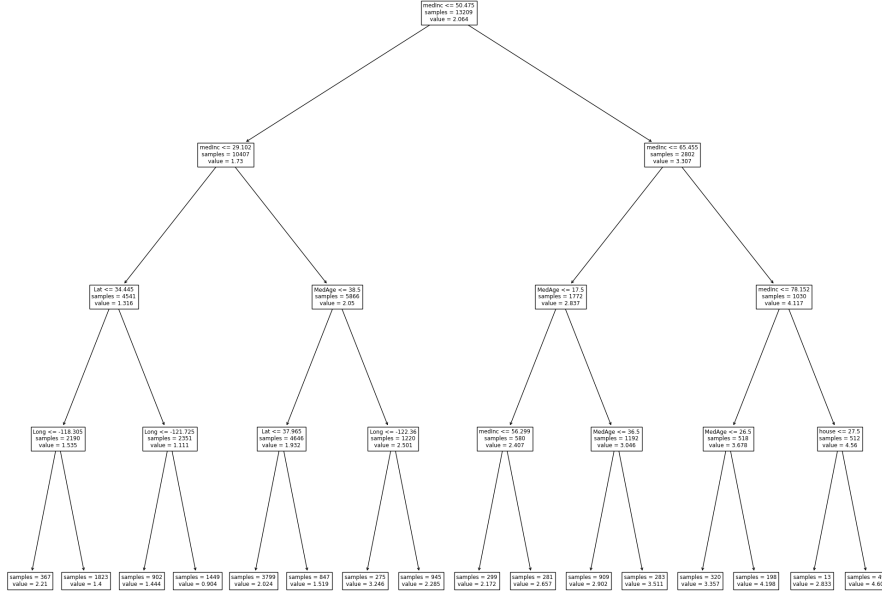


Figure 7. A visual representation of a regression tree of depth four trained on the *housing* dataset.

$$comb\left(\begin{bmatrix} 1 & 1 & 0 & 1 \end{bmatrix}\right) = \begin{bmatrix} 0 & 0 & 0 & 0 \\ 1 & 0 & 0 & 0 \\ 0 & 1 & 0 & 0 \\ 0 & 0 & 0 & 1 \\ 1 & 1 & 0 & 0 \\ 1 & 0 & 0 & 1 \\ 0 & 1 & 0 & 1 \\ 1 & 1 & 0 & 1 \end{bmatrix}$$

The function is useful for obtaining every combination of active feature for every hidden neuron (part (1) of the computation of Equation (9)).

Algorithm 1 does not directly returns SHAP values, but a $d \times d \times |L_1|$ tensor. In order to obtain the SHAP values, the tensor must be aggregated over the first dimension respecting the weighting or the terms $\left(\mathbb{E}_{X_{\overline{S \cup \{i\}}}}[f(\mathbf{x}_F)] - \mathbb{E}_{X_{\overline{S}}}[f(\mathbf{x}_F)]\right)$ following (2) in Equation (9). A $d \times |L_1|$ matrix is obtained. This matrix contains the relative importance of every feature - per hidden neuron. Now, whether the matrix is summed over the first or the second dimension will result, in the first case, of SHAP values for the hidden neurons (their relative importance in the model prediction) or, in the second case, in SHAP values for the features of the model (their relative importance).

Notice that Algorithm 1 can be generalized to deep neural networks, or networks tackling classification tasks. The main drawback being that the combinatorial term now depends on the total number of feature used by the model.

Algorithm 3 is in $O(m^2 \cdot d_0 \cdot d \cdot l \cdot 2^{d_0})$, where d is the network width and l is the network depth.

A.6. BGN Algorithms

Algorithms (4-6) respectively show the base BGN algorithm enhanced with Improvements (1, 2, 3). They allow a clear understanding of how the base algorithm changes with each one of them. Algorithm 7 depicts the complete BGN algorithm

Table 6. Comparison between trees of depth 3, 4 and 5 and 1-BANNs having correspondingly similar validation MSE on the *housing* dataset. We use the tree depth and the 1-BANN width as a metric for comparing their complexity, as well as the number of considered features of the models.

Pred.	compl.	Feature SHAP values								Valid. MSE
		Long	Lat	MedAge	totRooms	totBed	pop	house	medInc	
Net.	5	0	0	0.28	0	0.10	0	0	0.62	0.6358
Tree	3	0	0.10	0.14	0	0	0	0	0.76	0.6413
Net.	7	0	0	0.33	0	0	0.04	0.04	0.59	0.5849
Tree	4	0.10	0.16	0.13	0	0	0	0.01	0.60	0.5779
Net.	8	0	0.01	0.35	0	0.02	0.02	0.01	0.59	0.5020
Tree	5	0.16	0.18	0.11	0	0.01	0	0.01	0.54	0.5291

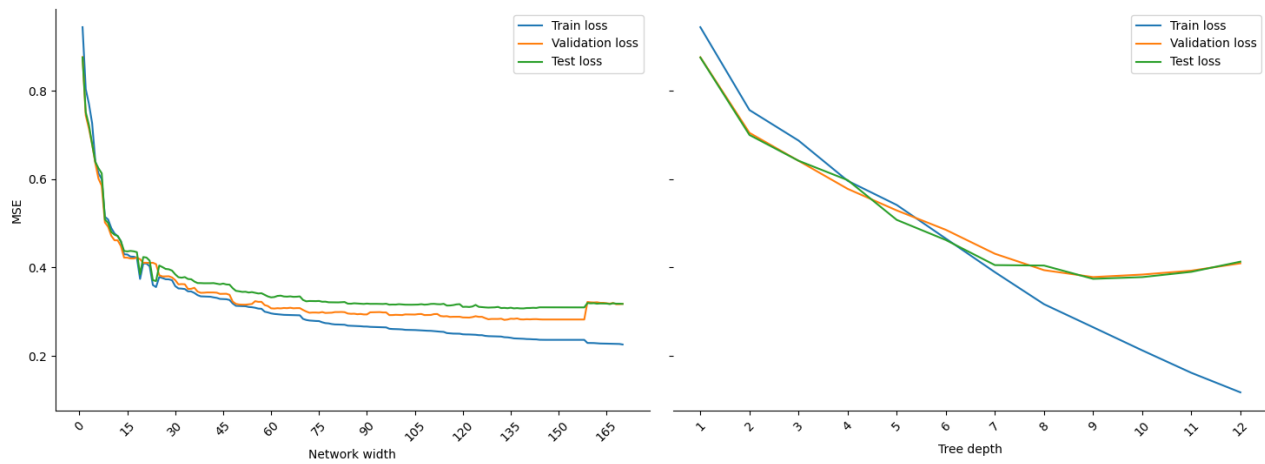


Figure 8. Mean performances over 5 random seeds on the *housing* dataset of a 1-BANN and a regression tree as a function, respectively, of the network width and the tree depth.

(base algorithm + every proposed improvement); it is the BGN algorithm that has been used in the experiments of section 7.

Algorithm 3 BANN SHAP

```

1: Input :  $\{\mathbf{x}_1, \dots, \mathbf{x}_m\}$ ,  $\mathbf{x} \in \mathbb{R}^d$ , the features of dataset
2:          $B$ , a BANN;  $\{\mathbf{W}_1, \dots, \mathbf{W}_l\}$ , its weights
3:  $\mathbf{R} = \mathbf{0}_{d \times d \times |L_1|}$ 
4:  $\mathbf{a} = \mathbb{1}_{\{\sum_i |\mathbf{w}_{1,i}| \neq 0\}}$ 
5:  $\mathbf{C} = \text{comb}(\mathbf{a})$ 
6: For  $i \in \{1, \dots, d\}$  such that  $(\exists j \mid c_{j,i} = 1)$ :
7:     For  $j \in \{1, \dots, |\mathbf{C}|\}$  such that  $c_{j,i} = 1$  :
8:         For  $\mathbf{x}, \mathbf{x}' \in S$  :
9:             If  $L_1(\mathbf{x}_{\mathbf{c} \setminus \{f\}} \cup \mathbf{x}'_{\mathbf{c} \setminus \{f\}}) \neq L_1(\mathbf{x}_{\mathbf{c}} \cup \mathbf{x}'_{\mathbf{c}})$  :
10:                  $\mathbf{r}_{i,|c_{j,i}|_1} = \mathbf{r}_{i,|c_{j,i}|_1} + \frac{\theta_{\mathbf{x},f}}{m} \odot \left| \sum_{k=1}^{d_i} \mathbf{w}_k \right|$ ,
11: with  $\theta_{\mathbf{x},f} = \left| B(\mathbf{x}_{\mathbf{c} \setminus \{f\}} \cup \mathbf{x}'_{\mathbf{c} \setminus \{f\}}) - B(\mathbf{x}_{\mathbf{c}} \cup \mathbf{x}'_{\mathbf{c}}) \right|$ 
12: Return  $\mathbf{R}$ 
    
```

Algorithm 4 Algorithm 2 + Improvement 1 (possibility to replace the hyperplanes)

```

1: Input :  $S = \{(\mathbf{x}_1, y_1), \dots, (\mathbf{x}_m, y_m)\}$ ,  $y \in \mathbb{R}$ ,  $\mathbf{x} \in \mathbb{R}^d$ , a dataset;
2:          $T$ , a number of iteration; Heuristic( $\cdot$ ), a method for placing hyperplanes
3: Set  $\mathbf{r}^{(1)} = \mathbf{y} = (y_1, \dots, y_m)$ 
4: For  $t = 1, \dots, T$  :
5:      $\mathbf{w}_t, b_t = \text{Heuristic}(S^{(t)})$ , where  $S^{(t)} = \{(\mathbf{x}_1, r_1^{(t)}), \dots, (\mathbf{x}_m, r_m^{(t)})\}$ 
6:      $c_t, d_t = \frac{1}{2}(\rho_+^{(t;t)} - \rho_-^{(t;t)})$ ,  $\frac{1}{2}(\rho_+^{(t;t)} + \rho_-^{(t;t)})$ , with  $\rho_{\pm}^{(t;k)} = \frac{\sum_{i:\text{sgn}(\mathbf{x}_i \cdot \mathbf{w}_k + b_k) = \pm 1} r_i^{(t)}}{\sum_{i:\text{sgn}(\mathbf{x}_i \cdot \mathbf{w}_k + b_k) = \pm 1} 1}$ 
7:      $r_i^{(t+1)} = r_i^{(t)} - c_t \text{sgn}(\mathbf{w}_t \cdot \mathbf{x}_i + b_t) - d_t \quad \forall i \in \{1, \dots, m\}$ 
8:     If  $t > 1$ :
9:          $k = 0$ 
10:    While  $Q(BGN_t, S)$  diminishes And  $k < t$ :
11:         $k = k + 1$ 
12:         $r_i^{(t)} = r_i^{(t)} + c_k \text{sgn}(\mathbf{w}_k \cdot \mathbf{x}_i + b_k) + d_k \quad \forall i \in \{1, \dots, m\}$ 
13:         $\mathbf{w}_k, b_k = \text{Heuristic}(S^{(t)})$ 
14:         $c_k, d_k = \frac{1}{2}(\rho_+^{(t;k)} - \rho_-^{(t;k)})$ ,  $\frac{1}{2}(\rho_+^{(t;k)} + \rho_-^{(t;k)})$ 
15:         $r_i^{(t)} = r_i^{(t)} - c_k \text{sgn}(\mathbf{w}_k \cdot \mathbf{x}_i + b_k) - d_k \quad \forall i \in \{1, \dots, m\}$ 
16: Output :  $BGN_T(\mathbf{x}) = \sum_{t=1}^T c_t \text{sgn}(\mathbf{w}_t \cdot \mathbf{x} + b_t) + d_t$ 
    
```

Algorithm 5 Algorithm 2 + Improvement 2 (multivariate tasks)

```

1: Input :  $S = \{(\mathbf{x}_1, \mathbf{y}_1), \dots, (\mathbf{x}_m, \mathbf{y}_m)\}$ ,  $\mathbf{y} \in \mathbb{R}^k$ ,  $\mathbf{x} \in \mathbb{R}^d$ , a dataset
2:          $T$ , a number of iteration; Heuristic( $\cdot$ ), a method for placing hyperplanes
3: Set  $r_{i,j}^{(1)} = (y_{1,j}, \dots, y_{m,j}) \forall i \in \{1, \dots, m\}, j \in \{1, \dots, k\}$ 
4: For  $t = 1, \dots, T$  :
5:      $S_j^{(t)} = \{(\mathbf{x}_1, r_{1,j}^{(t)}), \dots, (\mathbf{x}_m, r_{m,j}^{(t)})\} \forall j \in \{1, \dots, k\}$ 
6:      $S^{*(t)} = \bigcup_{j=1}^k S_j^{(t)}$ 
7:      $\mathbf{w}_t, b_t = \text{Heuristic}(S^{*(t)})$ 
8:      $c_{t,j}, d_{t,j} = \frac{1}{2}(\rho_{j+}^{(t)} - \rho_{j-}^{(t)})$ ,  $\frac{1}{2}(\rho_{j+}^{(t)} + \rho_{j-}^{(t)}) \forall j \in \{1, \dots, k\}$ ,
9:     with  $\rho_{j\pm}^{(t)} = \frac{\sum_{i:\text{sgn}(\mathbf{x}_i \cdot \mathbf{w}_t + b_t) = \pm 1} r_{i,j}^{(t)}}{\sum_{i:\text{sgn}(\mathbf{x}_i \cdot \mathbf{w}_t + b_t) = \pm 1} 1}$ 
10:     $r_{i,j}^{(t+1)} = r_{i,j}^{(t)} - c_{t,j} \text{sgn}(\mathbf{w}_t \cdot \mathbf{x}_i + b_t) - d_{t,j} \quad \forall i \in \{1, \dots, m\}, j \in \{1, \dots, k\}$ 
11: Output :  $BGN_T(\mathbf{x}) = \sum_{t=1}^T \mathbf{c}_t \text{sgn}(\mathbf{w}_t \cdot \mathbf{x} + b_t) + \mathbf{d}_t$ 
    
```

Algorithm 6 Algorithm 2 + Improvement 3 (deep neural networks building)

- 1: **Input** : $S = \{(\mathbf{x}_1, y_1), \dots, (\mathbf{x}_m, y_m)\}$, $y \in \mathbb{R}$, $\mathbf{x} \in \mathbb{R}^d$, a dataset
- 2: T , a number of iteration; Heuristic(\cdot), a method for placing hyperplanes
- 3: Set $\mathbf{r}^{(1)} = \mathbf{y} = (y_1, \dots, y_m)$
- 4: Set $\{\mathbf{x}_i^{(1)}\}_{i=1}^m = \{\mathbf{x}_i\}_{i=1}^m$
- 5: **For** $k = 1, \dots, l-1$:
- 6: **For** $t = 1, \dots, T$:
- 7: $\mathbf{w}_{k,t}, b_{k,t} = \text{Heuristic}(S^{(k,t)})$, where $S^{(k,t)} = \{(\mathbf{x}_1^{(k)}, r_1^{(t)}), \dots, (\mathbf{x}_m^{(k)}, r_m^{(t)})\}$
- 8: $c_t, d_t = \frac{1}{2} (\rho_+^{(k,t)} - \rho_-^{(k,t)})$, $\frac{1}{2} (\rho_+^{(k,t)} + \rho_-^{(k,t)})$; $\rho_{\pm}^{(k,t)} = \frac{\sum_{i: \text{sgn}(\mathbf{x}_i^{(k)} \cdot \mathbf{w}_{k,t} + b_{k,t}) = \pm 1} r_i^{(t)}}{\sum_{i: \text{sgn}(\mathbf{x}_i^{(k)} \cdot \mathbf{w}_{k,t} + b_{k,t}) = \pm 1} 1}$
- 9: $r_i^{(t+1)} = r_i^{(t)} - c_t \text{sgn}(\mathbf{w}_{k,t} \cdot \mathbf{x}_i^{(k)} + b_{k,t}) - d_t \quad \forall i \in \{1, \dots, m\}$
- 10: $\mathbf{x}_i^{(k+1)} = (L_k \circ \dots \circ L_1)(\mathbf{x}_i) \forall i \in \{1, \dots, m\}$
- 11: **Output** : $BGN_T(\mathbf{x}) = \sum_{t=1}^T c_t (L_{l-1} \circ \dots \circ L_1)(\mathbf{x}) + d_t$

Algorithm 7 The complete BGN algorithm

- 1: **Input** : $S = \{(\mathbf{x}_1, \mathbf{y}_1), \dots, (\mathbf{x}_m, \mathbf{y}_m)\}$, $\mathbf{y} \in \mathbb{R}^k$, $\mathbf{x} \in \mathbb{R}^d$, a dataset
- 2: T , a number of iteration; Heuristic(\cdot), a method for placing hyperplanes
- 3: Set $r_{i,j}^{(1)} = (y_{1,j}, \dots, y_{m,j}) \forall i \in \{1, \dots, m\}, j \in \{1, \dots, k\}$
- 4: Set $\{\mathbf{x}_i^{(1)}\}_{i=1}^m = \{\mathbf{x}_i\}_{i=1}^m$
- 5: **For** $z = 1, \dots, l-1$:
- 6: **For** $t = 1, \dots, T$:
- 7: $S_j^{(z,t)} = \{(\mathbf{x}_1^{(z)}, r_{1,j}^{(t)}), \dots, (\mathbf{x}_m^{(z)}, r_{m,j}^{(t)})\} \forall j \in \{1, \dots, k\}$
- 8: $S^{*(z,t)} = \bigcup_{j=1}^k S_j^{(z,t)}$
- 9: $\mathbf{w}_{z,t}, b_{z,t} = \text{Heuristic}(S^{*(z,t)})$
- 10: $c_{t,j}, d_{t,j} = \frac{1}{2} (\rho_{j+}^{(z,t;t)} - \rho_{j-}^{(z,t;t)})$, $\frac{1}{2} (\rho_{j+}^{(z,t;t)} + \rho_{j-}^{(z,t;t)}) \quad \forall j \in \{1, \dots, k\}$,
- 11: with $\rho_{j\pm}^{(z,t;p)} = \frac{\sum_{i: \text{sgn}(\mathbf{x}_i^{(z)} \cdot \mathbf{w}_{z,t} + b_{z,t}) = \pm 1} r_{i,j}^{(t)}}{\sum_{i: \text{sgn}(\mathbf{x}_i^{(z)} \cdot \mathbf{w}_{z,t} + b_{z,t}) = \pm 1} 1}$
- 12: $r_{i,j}^{(t+1)} = r_{i,j}^{(t)} - c_{t,j} \text{sgn}(\mathbf{w}_{z,t} \cdot \mathbf{x}_i^{(z)} + b_{z,t}) - d_{t,j} \quad \forall i \in \{1, \dots, m\}, j \in \{1, \dots, k\}$
- 13: **If** $t > 1$:
- 14: $p = 0$
- 15: **While** $Q(BGN_t, S)$ diminishes **And** $p < t$:
- 16: $p = p + 1$
- 17: $r_{i,j}^{(t)} = r_{i,j}^{(t)} + c_{p,j} \text{sgn}(\mathbf{w}_{z,p} \cdot \mathbf{x}_i^{(z)} + b_{z,p}) + d_{p,j} \quad \forall i \in \{1, \dots, m\}, j \in \{1, \dots, k\}$
- 18: $\mathbf{w}_{z,p}, b_{z,p} = \text{Heuristic}(S^{*(z,t)})$
- 19: $c_{p,j}, d_{p,j} = \frac{1}{2} (\rho_{j+}^{(z,t;p)} - \rho_{j-}^{(z,t;p)})$, $\frac{1}{2} (\rho_{j+}^{(z,t;p)} + \rho_{j-}^{(z,t;p)}) \quad \forall j \in \{1, \dots, k\}$
- 20: $r_{i,j}^{(t)} = r_{i,j}^{(t)} - c_{p,j} \text{sgn}(\mathbf{w}_{z,p} \cdot \mathbf{x}_i^{(z)} + b_{z,p}) - d_{p,j} \quad \forall i \in \{1, \dots, m\}, j \in \{1, \dots, k\}$
- 21: $\mathbf{x}_i^{(z+1)} = (L_z \circ \dots \circ L_1)(\mathbf{x}_i) \forall i \in \{1, \dots, m\}$
- 22: **Output** : $BGN_T(\mathbf{x}) = \sum_{t=1}^T \mathbf{c}_t (L_{l-1} \circ \dots \circ L_1)(\mathbf{x}) + \mathbf{d}_t$

A.7. Sobolev spaces

We denote a Sobolev space $\mathcal{W}^{n,p}([0,1]^d)$, where $n, d \in \mathbb{N}^*$, $p \in [1, \infty)$, defined as the space of functions on $[0,1]^d$ lying in L^p , along with their weak derivatives up to an order n :

$$\mathcal{W}^{n,p}([0,1]^d) = \{f \in L^p([0,1]^d) \mid \forall \mathbf{n} \text{ such that } |\mathbf{n}| \leq n, D^{\mathbf{n}} f \in L^p([0,1]^d)\},$$

where $\mathbf{n} \in \mathbb{N}^{*d}$, $|\mathbf{n}| = \sum_i^d n_i$, $D^{\mathbf{n}}f$ is a weak derivative of f and L^p denotes a Lebesgue space. We focus on $\mathcal{W}^{n,\infty}([0,1]^d)$, where the functions from that space have a norm that is defined as follows :

$$\begin{aligned} \|f\|_{\mathcal{W}^{n,\infty}} &= \lim_{p \rightarrow +\infty} \left(\sum_{|\mathbf{n}| \leq n} \|D^{\mathbf{n}}u\|_{L^p}^p \right)^{1/p} \\ &= \max_{\mathbf{n}:|\mathbf{n}| \leq n} \sup_{\mathbf{x} \in [0,1]^d} \text{ess } |D^{\mathbf{n}}f(\mathbf{x})|. \end{aligned}$$

An intuitive way to define a Sobolev space $\mathcal{W}^{n,\infty}([0,1]^d)$ is to see it as the space of functions in $C^{n-1}([0,1]^d)$ such that all their derivatives of order $n-1$ are Lipschitz continuous. In our results, we consider the unit ball $F_{n,d}$ of functions from $\mathcal{W}^{n,\infty}([0,1]^d)$ a norm upper bounded by 1:

$$F_{n,d} = \{f \in \mathcal{W}^{n,\infty}([0,1]^d) : \|f\|_{\mathcal{W}^{n,\infty}([0,1]^d)} \leq 1\}. \quad (10)$$

A.8. On why it makes sens to use (regularized) linear regression to parametrize the hidden neurons of BANNs for regression tasks

One of the claim that was made in the paper is that the BGN algorithm has solid theoretical groundings. Therefore, how can we explain the use of (regularized) linear regression for parametrizing the neurons of the BANNs? In what way does it makes sens and why does it work?

Let's consider the first hidden layer building. Adding a new neuron consist in adding a hyperplane in the input space. A hyperplane is parametrized by a vector to which it is orthogonal, plus a bias. Therefore, using linear regression to parametrize the hyperplane consists in directly using the direction toward which the linear predictor is pointing to parametrize the "orthogonal vector".

We saw that the hyperplane must, in order to obtain good empirical results, separates the input space in a way such that the term of Equation (8) is the smallest possible. We saw that this equation corresponds to the weighted sum of the variances of the points in both resulting regions; therefore, the hyperplane has to separates points with "high-valued labels" to those having "small-values labels".

Using linear regression in order to parametrize the hyperplane makes sens because the resulting vector will indicates a direction in which, in the input space, the labels grow. Using this direction to orientate the hyperplane than surely is a good way to separates points with "high-valued labels" to those having "small-values labels".

B. On the sparseness of BGN predictors

The sparseness of the predictors the BGN yields has been discussed in the paper, but not empirically supported. Two experiments have been conducted in order to demonstrate it. On two different datasets, networks with hidden layers of width respectively 100-100-20 and 100-65 have been built. Figure 9 and Figure 10 clearly show that the BGN predictors are composed of many 0-valued parameters, meaning that only the relevant parameters are non-zeros. Also, those two figures highlight the fact that BGN predictors are consistent; their number of parameters are quite stable.

C. Mathematical results

C.1. Proof of Proposition 1

Proposition 1. *Let B be a BANN parametrized by $\{\mathbf{W}_k, \mathbf{b}_k\}_{k=1}^l$ such that its activation functions are f_{t,h_1,h_2} on layers L_1 to L_{l-1} and the identity function on layer L_l . The same goes for B^* , having binary functions f_{t^*,h_1^*,h_2^*} . For all $t, h_1, h_2, t^*, h_1^*, h_2^* \in \mathbb{R}$, $h_1 > h_2$ and $h_1^* > h_2^*$, there exist weights and biases $\{\mathbf{W}_k^*, \mathbf{b}_k^*\}_{k=1}^l$ parametrizing B^* such that*

(i) B^* has the same architecture as B ;

(ii) $B^*(\mathbf{x}) = B(\mathbf{x}) \forall \mathbf{x} \in \mathbb{R}^{d_0}$;

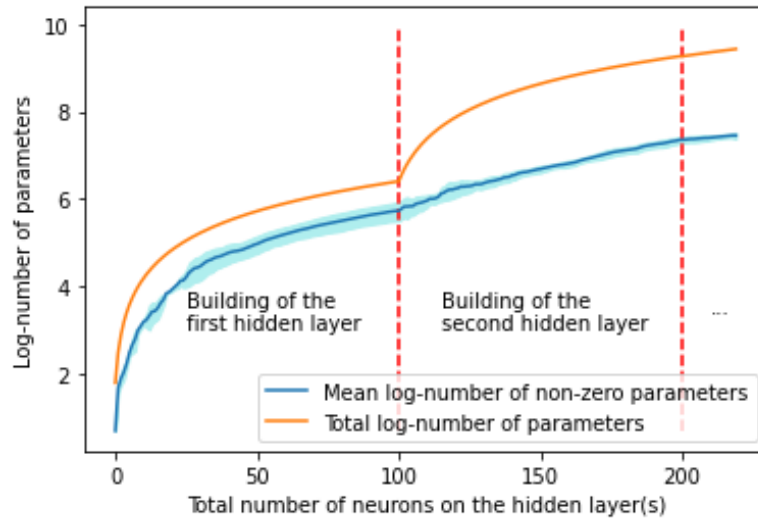


Figure 9. Mean and standard deviation over three repetitions of the number of non-zero parameters of the predictor yielded by BGN over its training on the Carbon nanotubes dataset versus the maximum number of parameter a NN with a similar architecture could have.

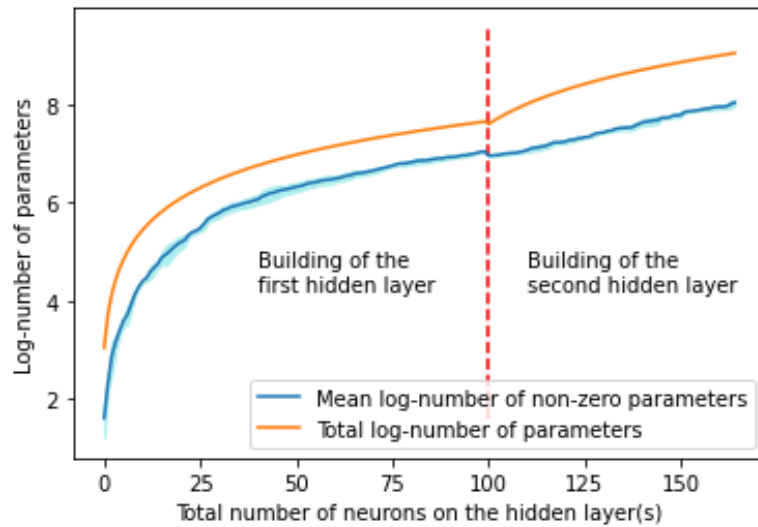


Figure 10. Mean and standard deviation over three repetitions of the number of non-zero parameters of the predictor yielded by BGN over its training on the Hungarian chickenpox cases dataset versus the maximum number of parameter a NN with a similar architecture could have.

$$(iii) \mathbf{W}_k^* = \begin{cases} \mathbf{W}_k & \text{if } k = 1, \\ \mathbf{W}_k \frac{h_1 - h_2}{h_1^* - h_2^*} & \text{if } 1 < k \leq l, \end{cases} \quad \mathbf{b}_k^* = \begin{cases} \mathbf{b}_k + \delta_t & \text{if } k = 1, \\ \mathbf{b}_k - \mathbf{c}_k + \delta_t & \text{if } 1 < k < l, \\ \mathbf{b}_k - \mathbf{c}_k & \text{if } k = l, \end{cases}$$

with $\delta_t = t^* - t$ and $\mathbf{c}_k = \frac{h_1 h_2^* - h_1^* h_2}{h_1^* - h_2^*} \left(\sum_j \mathbf{w}_{k,j} \right) \left(\sum_j \mathbf{w}_{k,j} \right)$.

Proof. The proof relies on finding weights and biases $\{\mathbf{W}_k^*, \mathbf{b}_k^*\}_{k=1}^l$ such that $B^*(\mathbf{x}) = B(\mathbf{x}) \forall \mathbf{x} \in \mathbb{R}^{d_0}$. To do so, we will ensure that $\{\mathbf{W}_k^*, \mathbf{b}_k^*\}_{k=1}^l$ are such that the input and output of every binary activation function is the same in both networks. We will first tackle the single-hidden layer case before extending it to deep binary activated neural networks.

In order to lighten the notation, we denote $f = f_{t,h_1,h_2}$ and $f^* = f_{t^*,h_1^*,h_2^*}$.

First of all, knowing that $h_1^* - h_2^* \neq 0$:

$$h_1 = \frac{h_1 - h_2}{h_1^* - h_2^*} h_1^* - \left(\frac{h_1 - h_2}{h_1^* - h_2^*} h_1^* - h_1 \right) = ah_1^* - k_1,$$

$$h_2 = \frac{h_1 - h_2}{h_1^* - h_2^*} h_2^* - \left(\frac{h_1 - h_2}{h_1^* - h_2^*} h_2^* - h_2 \right) = ah_2^* - k_2,$$

Let's demonstrate that $k_1 = k_2$:

$$\begin{aligned} h_1 - h_2 &= h_1 - h_2, \\ &= (h_1^* - h_2^*) \frac{h_1 - h_2}{h_1^* - h_2^*}, \\ &= h_1^* \frac{h_1 - h_2}{h_1^* - h_2^*} - h_2^* \frac{h_1 - h_2}{h_1^* - h_2^*}, \\ \Rightarrow \frac{h_1 - h_2}{h_1^* - h_2^*} h_2^* - h_2 &= \frac{h_1 - h_2}{h_1^* - h_2^*} h_1^* - h_1 \\ &\Rightarrow k_1 = k_2. \end{aligned}$$

By setting $k = k_1 = k_2 = \frac{h_1 h_2^* - h_1^* h_2}{h_1^* - h_2^*} \left(\sum_j \mathbf{w}_{k,j} \right)$ and $\delta = t^* - t$, we have the following relations between the parametrization of the binary functions from B of the one from B^* :

$$t = t^* - \delta, \quad h_1 = ah_1^* - k, \quad h_2 = ah_2^* - k.$$

where δ , a and k are known constants. Let us consider the first layer of the networks. In order to obtain $B^*(\mathbf{x}) = B(\mathbf{x}) \forall \mathbf{x} \in \mathbb{R}^{d_0}$, we must have the following relation:

$$L_1^*(w_{1,i,j}^* x + b_{1,i}^*) = \begin{cases} h_1^* & \text{if } L_1(w_{1,i,j} x + b_{1,i}) = h_1, \forall i \in d_1, j \in d_0. \\ h_2^* & \text{if } L_1(w_{1,i,j} x + b_{1,i}) = h_2, \end{cases} \quad (11)$$

Looking at Equation (12), we notice that in network B^* , if $\mathbf{b}_1^* = \mathbf{b}_1 + \delta$ and $\mathbf{W}_1^* = \mathbf{W}_1$, then Equation (11) holds.

$$\begin{aligned} \forall i \in d_1, j \in d_0 : f^* \left(\underbrace{w_{1,i,j}}_{w_{1,i,j}} x + \underbrace{b_{1,i}}_{b_{1,i}} + \delta \right) &= \begin{cases} h_1^* & \text{if } w_{1,i,j} x + b_{1,i} + \delta < t^*, \\ h_2^* & \text{otherwise,} \end{cases} \\ &= \begin{cases} h_1^* & \text{if } w_{1,i,j} x + b_{1,i} < t, \\ h_2^* & \text{otherwise,} \end{cases} \\ &= \begin{cases} h_1^* & \text{if } L_1(w_{1,i,j} x + b_{1,i}) = h_1, \\ h_2^* & \text{if } L_1(w_{1,i,j} x + b_{1,i}) = h_2, \end{cases} \end{aligned} \quad (12)$$

We now have to set weights and biases of layer L_2 in network B^* , such that

$$\mathbf{W}_2 f(\mathbf{x}) + \mathbf{b}_2 = \mathbf{W}_2^* f^*(\mathbf{x}) + \mathbf{b}_2^*.$$

Doing so, we would have $B(\mathbf{x}) = B^*(\mathbf{x})$ for the single-hidden layer case. Let \mathbf{h} and \mathbf{h}^* be column vectors, the respective output of $f(\mathbf{x})$ and $f^*(\mathbf{x})$ for a given input \mathbf{x} .

$$\begin{aligned} \forall i \in d_2 : \mathbf{w}_{2,i} f(\mathbf{x}) + b_{2,i} &= \mathbf{w}_{2,i} \mathbf{h} + b_{2,i} \\ &= \mathbf{w}_{2,i} (a\mathbf{h}^* - k) + b_{2,i} \\ &= a\mathbf{w}_{2,i} \mathbf{h}^* - k \left(\underbrace{\sum_j w_{2,i,j}}_{\hat{w}_2} \right) + b_{2,i} \\ &= a\mathbf{w}_{2,i} f^*(\mathbf{x}) - k\hat{w}_2 + b_{2,i} \\ &= \mathbf{w}_{2,i}^* f^*(\mathbf{x}) + b_{2,i}^* \end{aligned}$$

We now have that $B(\mathbf{x}) = B^*(\mathbf{x})$ holds for single-hidden layer networks if $\{\mathbf{W}_i^*, \mathbf{b}_i^*\}_{i=1}^2$ are set as follows:

$$\begin{aligned} \mathbf{W}_i^* &= \begin{cases} \mathbf{W}_i & \text{if } i = 1, \\ a\mathbf{W}_i & \text{if } i = 2, \end{cases} \\ &= \begin{cases} \mathbf{W}_i & \text{if } i = 1, \\ \frac{h_1 - h_2}{h_1^* - h_2^*} \mathbf{W}_i & \text{if } i = 2, \end{cases} \\ \mathbf{b}_i^* &= \begin{cases} \mathbf{b}_i + \delta & \text{si } i = 1, \\ \mathbf{b}_i - k\hat{w}_2 & \text{if } i = 2, \end{cases} \\ &= \begin{cases} \mathbf{b}_i + (t^* - t) & \text{if } i = 1, \\ \mathbf{b}_i - \frac{h_1 h_2^* - h_1^* h_2}{h_1^* - h_2^*} \left(\sum_j \mathbf{w}_{k,j} \right) \left(\sum_j \mathbf{w}_{i,j} \right) & \text{if } i = 2. \end{cases} \end{aligned}$$

The generalisation to deep BANNs is made by considering that in order to obtain $B^*(\mathbf{x}) = B(\mathbf{x}) \forall \mathbf{x} \in \mathbb{R}^{d_0}$, we must have $L_{1:k}(\mathbf{x}) = L_{1:k}^*(\mathbf{x}) \forall k \in \{1, \dots, l\}, \mathbf{x} \in \mathbb{R}^{d_0}$. Until now, we have considered how to modify weights and biases $\{\mathbf{W}_i^*, \mathbf{b}_i^*\}_{i=1}^2$ so that $\mathbf{W}_2 L_1(\mathbf{x}) + \mathbf{b}_2 = \mathbf{W}_2^* L_1^*(\mathbf{x}) + \mathbf{b}_2^*$ given a same input \mathbf{x} . By iteratively modifying the weights and biases of the network the same way we did for a single-hidden layer BANN, we obtain

$$\begin{aligned} &\mathbf{x} = \mathbf{x} \\ \Rightarrow \underbrace{\mathbf{W}_2 f(\mathbf{W}_1 \mathbf{x} + \mathbf{b}_1)}_{L_1(\mathbf{x})} + \mathbf{b}_2 &= a \underbrace{\mathbf{W}_2 f^*(\mathbf{W}_1 \mathbf{x} + \mathbf{b}_1 + \delta)}_{L_1^*(\mathbf{x})} + \mathbf{b}_2 - k\hat{w}_2 \\ \Rightarrow \mathbf{W}_3 f(\mathbf{W}_2 L_1(\mathbf{x}) + \mathbf{b}_2) + \mathbf{b}_3 &= a \mathbf{W}_3 f^* \left(\underbrace{a \mathbf{W}_2 L_1^*(\mathbf{x})}_{\mathbf{W}_2^*} + \underbrace{\mathbf{b}_2 - k\hat{w}_2 + \delta}_{\mathbf{b}_2^*} \right) + \mathbf{b}_3 - k\hat{w}_3 \end{aligned}$$

By that last recursion, we obtain the following weights and biases $\{\mathbf{W}_k^*, \mathbf{b}_k^*\}_{k=1}^l$ for any network of depth $l, l \in \mathbb{N} \setminus \{0, 1\}$:

$$\begin{aligned} \mathbf{W}_i^* &= \begin{cases} \mathbf{W}_i & \text{if } i = 1, \\ a\mathbf{W}_i & \text{if } i \in \{2, \dots, l\}, \end{cases} \\ &= \begin{cases} \mathbf{W}_i & \text{if } i = 1, \\ \frac{h_1 - h_2}{h_1^* - h_2^*} \mathbf{W}_i & \text{if } i \in \{2, \dots, l\}, \end{cases} \end{aligned}$$

$$\mathbf{b}_i^* = \begin{cases} \mathbf{b}_i + \delta & \text{si } i = 1, \\ \mathbf{b}_i - k \left(\sum_j \mathbf{w}_{i,j} \right) + \delta & \text{if } i \in \{2, \dots, l-1\}, \\ \mathbf{b}_i - k \left(\sum_j \mathbf{w}_{i,j} \right) & \text{if } i = l, \end{cases}$$

$$= \begin{cases} \mathbf{b}_i + (t^* - t) & \text{if } i = 1, \\ \mathbf{b}_i - \frac{h_1 h_2^* - h_1^* h_2}{h_1^* - h_2^*} \left(\sum_j \mathbf{w}_{k,j} \right) \left(\sum_j \mathbf{w}_{i,j} \right) + (t^* - t) & \text{if } i \in \{2, \dots, l-1\}, \\ \mathbf{b}_i - \frac{h_1 h_2^* - h_1^* h_2}{h_1^* - h_2^*} \left(\sum_j \mathbf{w}_{k,j} \right) \left(\sum_j \mathbf{w}_{i,j} \right) & \text{if } i = l. \end{cases}$$

□

C.2. Proof of Propositions 2.1 and 2.2

Proposition 2.1. *Let B be a BANN of depth l . Let $Q(B, S)$ be the mean squared error of predictor B on dataset S and $\|\cdot\|$ be the Euclidean norm. Then*

$$Q(B, S) := \sum_{(\mathbf{x}, \mathbf{y}) \in S} \frac{\|B(\mathbf{x}) - \mathbf{y}\|^2}{m} \geq \sum_{j=1}^{d_l} \sum_{\mathbf{p} \in \mathcal{L}_{1:l-1}} \frac{|\mathbf{y}_{\mathbf{p},j}^{(l-1)}|}{m} \text{Var}(\mathbf{y}_{\mathbf{p},j}^{(l-1)}) \geq \dots \geq \sum_{j=1}^{d_1} \sum_{\mathbf{p} \in \mathcal{L}_1} \frac{|\mathbf{y}_{\mathbf{p},j}^{(1)}|}{m} \text{Var}(\mathbf{y}_{\mathbf{p},j}^{(1)}),$$

where $m = |S|$ and $\mathbf{y}_{\mathbf{p},j}^{(k)} = \{y_{i,j} \mid (\mathbf{x}_i, \mathbf{y}_i) \in S, (L_k \circ \dots \circ L_1)(\mathbf{x}_i) = \mathbf{p}\} \forall k \in \{1, \dots, l-1\}$.

Proof.

$$Q(B, S) = \sum_{(\mathbf{x}, \mathbf{y}) \in S} \frac{\|B(\mathbf{x}) - \mathbf{y}\|^2}{m} \tag{13}$$

$$= \frac{1}{m} \sum_{j=1}^{d_l} \sum_{(\mathbf{x}, \mathbf{y}) \in S} (B(\mathbf{x}) - y_j)^2 \tag{14}$$

$$= \frac{1}{m} \sum_{j=1}^{d_l} \sum_{(\mathbf{x}, \mathbf{y}) \in S} (\mathbf{w}_{l,j} \cdot L_{1:l-1}(\mathbf{x}) + b_{l,j} - y_j)^2 \tag{15}$$

$$= \frac{1}{m} \sum_{j=1}^{d_l} \sum_{\mathbf{p} \in \mathcal{L}_{1:l-1}} \sum_{\substack{(\mathbf{x}, \mathbf{y}) \in S \\ L_{1:l-1}(\mathbf{x}) = \mathbf{p}}} (\mathbf{w}_{l,j} \cdot \mathbf{p} + b_{l,j} - y_j)^2 \tag{16}$$

$$\geq \frac{1}{m} \sum_{j=1}^{d_l} \sum_{\mathbf{p} \in \mathcal{L}_{1:l-1}} \underset{\mathbf{w}, b}{\text{argmin}} \sum_{\substack{(\mathbf{x}, \mathbf{y}) \in S \\ L_{1:l-1}(\mathbf{x}) = \mathbf{p}}} (\mathbf{w} \cdot \mathbf{p} + b - y_j)^2 \tag{17}$$

$$= \sum_{j=1}^{d_l} \sum_{\mathbf{p} \in \mathcal{L}_{1:l-1}} \frac{|\mathbf{y}_{\mathbf{p},j}^{(l-1)}|}{m} \frac{1}{|\mathbf{y}_{\mathbf{p},j}^{(l-1)}|} \sum_{\substack{(\mathbf{x}, \mathbf{y}) \in S \\ L_{1:l-1}(\mathbf{x}) = \mathbf{p}}} \left(\overline{\mathbf{y}_{\mathbf{p},j}^{(l-1)}} - y_j \right)^2 \tag{18}$$

$$= \sum_{j=1}^{d_l} \sum_{\mathbf{p} \in \mathcal{L}_{1:l-1}} \frac{|\mathbf{y}_{\mathbf{p},j}^{(l-1)}|}{m} \text{Var}(\mathbf{y}_{\mathbf{p},j}^{(l-1)}) . \tag{19}$$

The inequality is obtained by considering different values for \mathbf{w} and b in each of the $|\mathcal{L}_{1:l-1}|$ regions, while they're fixed in a typical neural network. The predictor $\overline{\mathbf{y}}_{\mathbf{p},j}^{(l-1)}$ is the constant predictor minimizing the MSE on a given task: the mean of the labels to predict. We saw in section 4.2 that hidden layers L_2 to L_l regroup regions created by the preceding hidden layer. Using the fact that for two datasets S_1 and S_2 , we have

$$\min_c \left(\sum_{(\mathbf{x},y) \in S_1} (c - y_i)^2 + \sum_{(\mathbf{x},y) \in S_2} (c - y_i)^2 \right) \geq \min_c \sum_{(\mathbf{x},y) \in S_1} (c - y_i)^2 + \min_c \sum_{(\mathbf{x},y) \in S_2} (c - y_i)^2,$$

we obtain that $\forall k \in \{2, \dots, l-1\}$:

$$\sum_{j=1}^{d_l} \sum_{\mathbf{p} \in \mathcal{L}_{1:k}} \sum_{\substack{(\mathbf{x},\mathbf{y}) \in S \\ L_{1:k}(\mathbf{x})=\mathbf{p}}} \left(\overline{\mathbf{y}}_{\mathbf{p},j}^{(k)} - y_j \right)^2 \geq \sum_{j=1}^{d_l} \sum_{\mathbf{p} \in \mathcal{L}_{1:k-1}} \sum_{\substack{(\mathbf{x},\mathbf{y}) \in S \\ L_{1:k-1}(\mathbf{x})=\mathbf{p}}} \left(\overline{\mathbf{y}}_{\mathbf{p},j}^{(k-1)} - y_j \right)^2,$$

completing the proof. \square

Proposition 2.2 aims to bound, as it's been done in Proposition 2.1, the empirical loss obtained by a binary activated neural network, but this time on binary classification tasks and with the mean 0-1 loss. The proof is very similar to the one of Proposition 2.1:

Proposition 2.2. *Let B be a BANN of depth l . Let $Z(B, S)$ be the mean 0-1 error of predictor B on dataset $S = \{(\mathbf{x}_i, y_i)\}_{i=1}^m$, $y_i \in \{-1, 1\} \forall i \in \{1, \dots, m\}$. Let $I(\cdot)$ be the indicator function, where $I(a) = 1$ if a is true, 0 otherwise. Then*

$$Z(B, S) := \frac{1}{m} \sum_{(\mathbf{x},y) \in S} I(B(\mathbf{x}) \neq y) \geq \frac{1 - \sum_{\mathbf{p} \in \mathcal{L}_{1:l-1}} \frac{|\mathbf{y}_{\mathbf{p}}^{(l-1)}|}{m} \left| \overline{\mathbf{y}}_{\mathbf{p}}^{(l-1)} \right|}{2} \geq \dots \geq \frac{1 - \sum_{\mathbf{p} \in \mathcal{L}_1} \frac{|\mathbf{y}_{\mathbf{p}}^{(1)}|}{m} \left| \overline{\mathbf{y}}_{\mathbf{p}}^{(1)} \right|}{2},$$

where and $\mathbf{y}_{\mathbf{p},j}^{(k)} = \{y_{i,j} \mid (\mathbf{x}_i, \mathbf{y}_i) \in S, (L_k \circ \dots \circ L_1)(\mathbf{x}_i) = \mathbf{p}\} \forall k \in \{1, \dots, l-1\}$.

Proof.

$$Z(B, S) = \frac{1}{m} \sum_{(\mathbf{x},y) \in S} I(B(\mathbf{x}) \neq y) \tag{20}$$

$$= \frac{1}{m} \sum_{(\mathbf{x},\mathbf{y}) \in S} I(\text{sgn}(\mathbf{w}_l \cdot L_{1:l-1}(\mathbf{x}) + b_l) \neq y) \tag{21}$$

$$= \frac{1}{m} \sum_{\mathbf{p} \in \mathcal{L}_{1:l-1}} \sum_{\substack{(\mathbf{x},\mathbf{y}) \in S \\ L_{1:l-1}(\mathbf{x})=\mathbf{p}}} I(\text{sgn}(\mathbf{w}_l \cdot \mathbf{p} + b_l) \neq y) \tag{22}$$

$$\geq \frac{1}{m} \sum_{\mathbf{p} \in \mathcal{L}_{1:l-1}} \underset{\mathbf{w}, b}{\text{argmin}} \sum_{\substack{(\mathbf{x},\mathbf{y}) \in S \\ L_{1:l-1}(\mathbf{x})=\mathbf{p}}} I(\text{sgn}(\mathbf{w} \cdot \mathbf{p} + b) \neq y) \tag{23}$$

$$= \frac{1}{m} \sum_{\mathbf{p} \in \mathcal{L}_{1:l-1}} \sum_{\substack{(\mathbf{x},\mathbf{y}) \in S \\ L_{1:l-1}(\mathbf{x})=\mathbf{p}}} I\left(\text{sgn}\left(\overline{\mathbf{y}}_{\mathbf{p}}^{(l-1)}\right) \neq y\right) \tag{24}$$

$$= \frac{1}{2} \left(1 - \sum_{\mathbf{p} \in \mathcal{L}_{1:l-1}} \frac{|\mathbf{y}_{\mathbf{p}}^{(l-1)}|}{m} \left| \overline{\mathbf{y}}_{\mathbf{p}}^{(l-1)} \right| \right). \tag{25}$$

The rest of the proof follows that of Proposition 2.1. \square

We obtain similar quantity to minimize in both Proposition 2.1 and Proposition 2.2; in order to minimize a lower bound on the training loss, the hyperplanes have to be placed such that the points being grouped together have similar labels. In the classification case, it simply tells us that if points with very dissimilar labels are grouped together, necessarily, classification error will be made on several points of that group. In fact, another relation can be established; we know from Equation (8), when placing a neuron, in the regression context, the quantity to minimize in order to minimize the bound from Proposition 2.1; it can be rewritten as follows:

$$\begin{aligned}
 & \operatorname{argmin}_{\mathbf{w}, b} \left(\frac{|\mathbf{y}_{-1}|}{m} \operatorname{Var}(\mathbf{y}_{-1}) + \frac{|\mathbf{y}_{+1}|}{m} \operatorname{Var}(\mathbf{y}_{+1}) \right) \\
 &= \operatorname{argmin}_{\mathbf{w}, b} \left(\sum_{\substack{(\mathbf{x}, y) \in S \\ \mathbf{w} \cdot \mathbf{x} + b < 0}} (\bar{\mathbf{y}}_{-1} - y)^2 + \sum_{\substack{(\mathbf{x}, y) \in S \\ \mathbf{w} \cdot \mathbf{x} + b > 0}} (\bar{\mathbf{y}}_{+1} - y)^2 \right) \\
 &= \operatorname{argmin}_{\mathbf{w}, b} \left(\sum_{\substack{(\mathbf{x}, y) \in S \\ \mathbf{w} \cdot \mathbf{x} + b < 0}} y^2 - |\mathbf{y}_{-1}| \bar{\mathbf{y}}_{-1}^2 + \sum_{\substack{(\mathbf{x}, y) \in S \\ \mathbf{w} \cdot \mathbf{x} + b > 0}} y^2 - |\mathbf{y}_{+1}| \bar{\mathbf{y}}_{+1}^2 \right) \\
 &= \operatorname{argmin}_{\mathbf{w}, b} \left(-|\mathbf{y}_{-1}| \bar{\mathbf{y}}_{-1}^2 - |\mathbf{y}_{+1}| \bar{\mathbf{y}}_{+1}^2 \right) \\
 &= \operatorname{argmax}_{\mathbf{w}, b} \left(\frac{|\mathbf{y}_{-1}|}{m} \bar{\mathbf{y}}_{-1}^2 + \frac{|\mathbf{y}_{+1}|}{m} \bar{\mathbf{y}}_{+1}^2 \right).
 \end{aligned}$$

In the classification setting, from Proposition 2.2, we obtain these quantities to optimize:

$$\operatorname{argmin}_{\mathbf{w}, b} \frac{1}{2} \left(1 - \frac{|\mathbf{y}_{-1}|}{m} |\bar{\mathbf{y}}_{-1}| - \frac{|\mathbf{y}_{+1}|}{m} |\bar{\mathbf{y}}_{+1}| \right) = \operatorname{argmax}_{\mathbf{w}, b} \left(\frac{|\mathbf{y}_{-1}|}{m} |\bar{\mathbf{y}}_{-1}| + \frac{|\mathbf{y}_{+1}|}{m} |\bar{\mathbf{y}}_{+1}| \right).$$

In short, it seems like in the regression case, with MSE loss function, in order to minimize the bound from Proposition 2.1, when a hyperplane is placed, one must maximize the weighted sum of the **squared mean** (or minimize the variance) of the examples falling on each side of the hyperplane, whereas in the binary classification setting, with the 0-1 loss, in order to minimize the bound from Proposition 2.2, when a hyperplane is placed, one must maximize the weighted sum of the **absolute mean** of the examples falling on each side of the hyperplane. These results can be generalized to a whole layer.

C.3. Proof of Theorem 1 (i) and (ii)

The demonstration of Theorem 1 (i) and (ii) is done in three steps: we start by showing how binary activated neural networks (BANNs) can estimate a function g defined as follows: $g(x) = x^2$, $x \in [0, 1]$ (Proposition 2.2). Then, we take that first result in order to estimate the function $g(x, y) = xy$, $|x|, |y| < m$, with $m \in \mathbb{R}^*$ fixed (Proposition 2.2). Finally, we use those last two results as building blocks for estimating any function from $F_{n,d}$ (Theorem 1 (i) and (ii)). The first step is original, while the last two steps are adaptations of the work from Yarotsky (2017) to BANNs.

Proposition 2.2. *Let $\epsilon > 0$. There exists a fully connected binary activated neural network B approximating $g(x) = x^2$ on $x \in [0, 1]$ such that: (i) $\forall x \in [0, 1] : |g(x) - B(x)| \leq \epsilon$; (ii) B has only one hidden layer; (iii) the width of that hidden layer is in $O(\epsilon^{-1})$; (iv) $g(x) - B(x) = 0 \forall x \in \{0, 1\}$.*

Proof. The proof will be done in two parts: we show that there exists a non-continuous piece-wise linear function formed of r parallel lines $g^{(r)}(x)$ possessing the characteristic (iv), such that $|g(x) - g^{(r)}(x)| \leq (2r)^{-1} \forall x \in [0, 1]$; then, we show that there exists a fully connected BANN having characteristics (ii) and (iii) and being capable of constructing $g^{(r)}(x)$. By using $\epsilon = (2r)^{-1}$, the proof will be completed.

First, when estimating $g(x) = x^2$ on $[0, 1]$ with r parallel lines, in order to obtain the minimum approximation error, the lines must be such that (i) they're equidistant and (ii) that distance must be twice the maximum error. We will also need that (iii) on the bounds on the considered interval for x , the approximation error is null. With that configuration (see Figure 11), each line is, for some values of x , the best estimator of the function of interest.

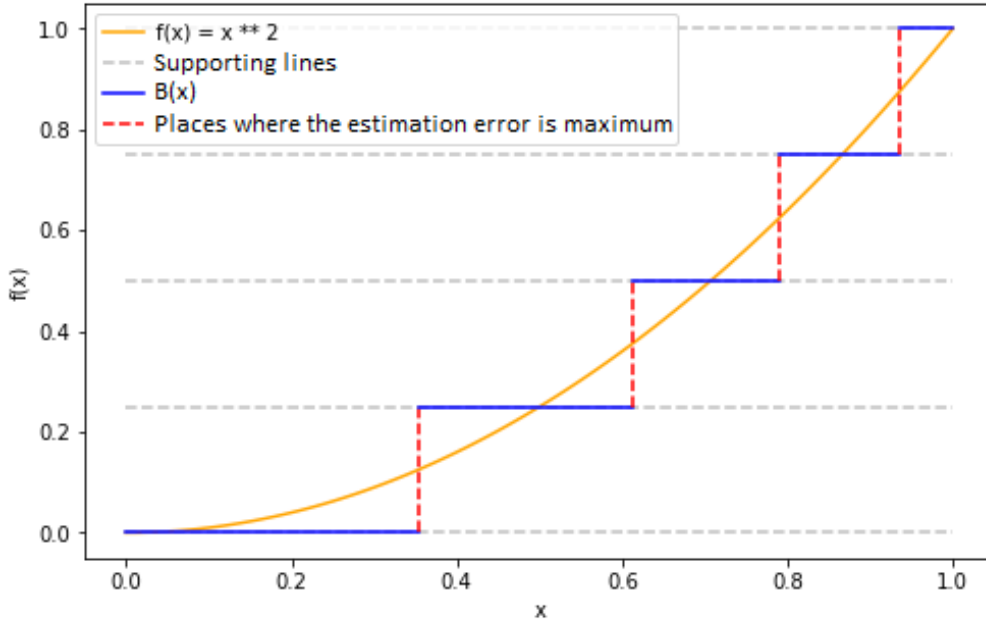
Estimation of $f(x) = x^2$ on $x \in [0,1]$ by a binary activated neural network B


Figure 11. Approximation of $f(x) = x^2$, $x \in [0, 1]$ by an ensemble of r parallel lines, corresponding to the output of a binary activated neural network.

When estimating function $g(x)$ with the line $g^{(1)}(x) = 0$, the maximum obtained error is 1; which is the same when considering the line $g^{(1)}(x) = 1$. These lines will be bounding $g(x)$: that last function is always between the two lines. When adding lines to the estimator (thus, $r > 2$), we uniformly place these lines between $g^{(1)}(x) = 0$ and $g^{(1)}(x) = 1$. The maximum error thus corresponds to 1 divided by $2r$: the space between each line is now $\frac{1}{r}$, thus two times the maximum error. We can then estimate $g(x) = x^2$ on $[0, 1]$ with an ensemble of r straight parallel lines and obtaining $|g(x) - g^{(r)}(x)| \leq \frac{1}{2r} = (2r)^{-1} \forall x \in [0, 1]$.

The ensemble of lines depicted on Figure 11 is a predictor that can be written as follows:

$$g^{(r)}(x) = b_0 - \sum_{i=0}^{2(r-2)} w_{2i} \mathbb{I}_{\{xw_{2i+1} - b_{i+1} > 0\}} \quad (26)$$

$$g^{(r)}(x) = (b_0 + 0.5) - \sum_{i=0}^{2(r-2)} \frac{w_{2i}}{2} \operatorname{sgn}(xw_{2i+1} - b_{i+1}). \quad (27)$$

Both Equations (26-27) present a particular form: it's a sum of terms being the result of the application of a binary function, each of them having as input a linear function of x . The output of the network presented on Figure 12 is similar to Equations (26-27). Indeed, it represents the output of a fully connected single-hidden layer BANN. Also, Equations (26-27) explicitly show how r directly affects the number of binary activation functions in the equations; r is thus proportional to the number of neurons in the hidden layer of the network. Also, ϵ is inversely proportional to r .

Since that configuration respects (ii) and (iii) when choosing $r = \lceil (2\epsilon)^{-1} \rceil$, the proof of Proposition 2.2 is completed. \square

Proposition 2.2. *Let $x, y \in \mathbb{R}$ and $m > 0$. There exists a fully connected BANN $\times'_m : \mathbb{R}^2 \mapsto \mathbb{R}$, such that (i) $\forall |x|, |y| \leq m$, the error $\epsilon_{\times'} = |\times'(x, y) - xy|$ is upper bounded by ϵ ; (ii) the depth of the network is constant; (iii) the width of the first hidden layer of the network is in $O(m^2\epsilon^{-1})$; (iv) $\epsilon_{\times'} = 0$ if $x = 0 \vee y = 0$.*

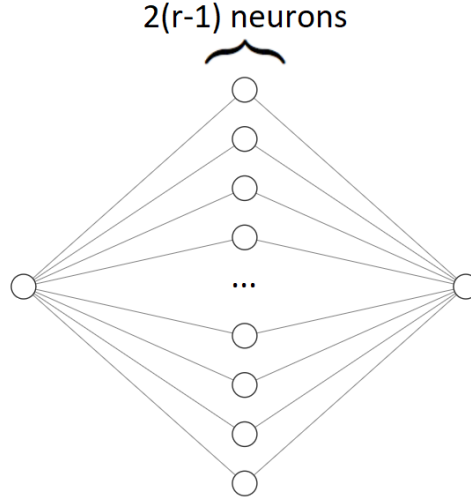


Figure 12. A shallow but wide neural network; the architecture of a BANN having an output as presented in Equations (26-27).

Proof. Let $g_\delta^{(r)}(x)$ be the approximation function from Proposition 2.2, where $\epsilon_{g_\delta^{(r)}} \leq \delta$. The proof will make use of the demonstration of Proposition 2.2 and the fact that $xy = \frac{(x+y)^2}{2} - \frac{x^2}{2} - \frac{y^2}{2}$. We have that

$$\times'_m(x, y) = m^2 \left(2g_\delta^{(r)} \left(\frac{|x+y|}{m} \right) - \frac{1}{2}g_\delta^{(r)} \left(\frac{|x|}{m} \right) - \frac{1}{2}g_\delta^{(r)} \left(\frac{|y|}{m} \right) \right). \quad (28)$$

The upper bound of $\times'_m(x, y)$ as a function of δ can easily be found:

$$\begin{aligned} \epsilon_{\times'(x,y)} &\leq m^2 \left(2\delta + \frac{1}{2}\delta + \frac{1}{2}\delta \right) \\ &= 3m^2\delta. \end{aligned}$$

Equation (28) indicates that, in the end, the network estimating the function $g(x, y) = xy$ takes the form of a weighted sum of three sub-networks. Since the global network is constituted of a constant number of sub-networks, we have that (ii) is verified. Also, Equation (28) confirms that (iv) is verified, considering that Proposition 2.2 indicates that the error, on bounds of the considered interval for the input of the network, is 0.

As for (i), it is sufficient to choose $\delta = \frac{\epsilon}{3}$ for it to be verified. Finally, since the width of each sub-network is in $O(\epsilon^{-1})$, (iii) is also verified. \square

Theorem 1 (i) and (ii) For $n, d \in \mathbb{N}^*$, there exists a fully connected BANN (i) capable of estimating any function from $F_{n,d}$ with absolute error upper bounded by ϵ ; (ii) having a first hidden layer with width in $O(c\epsilon^{-(d/n+1)})$, where c is a constant depending on n and d , (iii) and having a constant depth.

Proof. Let f be a function from $F_{n,d}$. The proof will be done in two main parts: first, we approximate f by f_1 , a combination of Taylor polynomials of order $n-1$ and one-dimensional piecewise linear functions while finding the error bound. We finish the proof by estimating f_1 by g_1 , a binary activated feed-forward neural network, using Proposition 2.2.

We will need the use of a partition of unity on $[0,1]^d$: $\sum_{\mathbf{m}} \psi_{\mathbf{m}} \equiv 1$. Here, $\mathbf{x} \in [0,1]^d$, $\mathbf{m} = (m_1, \dots, m_d) \in \{0, 1, \dots, N\}^d$ and $N \in \mathbb{N}^*$. $\psi_{\mathbf{m}}(\mathbf{x})$ is defined as follows:

$$\psi_{\mathbf{m}}(\mathbf{x}) = \prod_{k=1}^d h(3Nx_k - 3m_k),$$

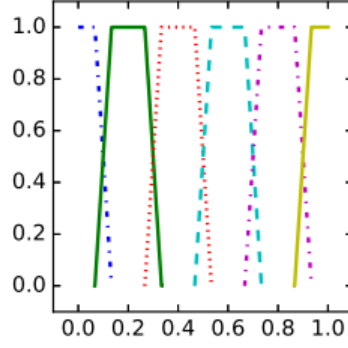


Figure 13. Figure taken from Yarotsky (2017): Functions $(\psi_{\mathbf{m}})_{\mathbf{m}=0}^5$ forming a partition of unity for $d = 1$, $N = 5$.

and

$$h(x) = \begin{cases} 1, & |x| \leq 1 \\ 2 - |x|, & 1 < |x| < 2 \\ 0, & |x| \geq 2 \end{cases}.$$

See Figure 13 for an example of $\psi_{\mathbf{m}}(\mathbf{x})$. Note that $\|h\|_{\infty} = 1$ and $\|\psi_{\mathbf{m}}\|_{\infty} = 1 \forall \mathbf{m}$; that is:

$$\sup_{\mathbf{x}} h = \sup_{\mathbf{x}} \psi_{\mathbf{m}} = 1 \forall \mathbf{m}.$$

Also, we have that

$$\text{supp } \psi_{\mathbf{m}} \subset \left\{ \mathbf{x} : \left| x_k - \frac{m_k}{N} \right| < \frac{1}{N} \forall k \right\}, \quad (29)$$

since $\text{supp } \psi_{\mathbf{m}} = \{ \mathbf{x} \in [0,1]^d \mid \psi_{\mathbf{m}}(\mathbf{x}) \neq 0 \}$ and that $\psi_{\mathbf{m}}(\mathbf{x}) = 0$ when at least one component x_k is such that $|x_k - \frac{m_k}{N}| \geq \frac{2}{3N}$.

Now, for all \mathbf{m} , consider the order $n - 1$ Taylor polynomial for the function f at $x = \frac{\mathbf{m}}{N}$:

$$P_{\mathbf{m}}(\mathbf{x}) = \sum_{\mathbf{n}: |\mathbf{n}| < n} \frac{D^{\mathbf{n}} f}{\mathbf{n}!} \Big|_{\mathbf{x} = \frac{\mathbf{m}}{N}} \left(\mathbf{x} - \frac{\mathbf{m}}{N} \right)^{\mathbf{n}}.$$

We will use the usual conventions $\mathbf{n}! = \prod_{k=1}^d n_k!$ and $(\mathbf{x} - \frac{\mathbf{m}}{N})^{\mathbf{n}} = \prod_{k=1}^d (x_k - \frac{m_k}{N})^{n_k}$. We get an approximation f_1 of f using $P_{\mathbf{m}}$ and $\psi_{\mathbf{m}}$ as follows:

$$f_1 = \sum_{\mathbf{m} \in \{0, \dots, N\}^d} \psi_{\mathbf{m}} P_{\mathbf{m}}.$$

Therefore, f_1 is a sum of $(N + 1)^d$ terms. Each of them is a multiplication of a linear term ($\psi_{\mathbf{m}}$) and a sum of d^n terms ($P_{\mathbf{m}}$). Let's bound the approximation error of f_1 :

$$\begin{aligned}
 |f(\mathbf{x}) - f_1(\mathbf{x})| &= \left| \sum_{\mathbf{m}} \psi_{\mathbf{m}}(\mathbf{x})(f(\mathbf{x}) - P_{\mathbf{m}}(\mathbf{x})) \right| \\
 &\leq \sum_{\mathbf{m}} |\psi_{\mathbf{m}}(f(\mathbf{x}) - P_{\mathbf{m}}(\mathbf{x}))| \\
 &\leq \sum_{\mathbf{m}: |x_k - \frac{m_k}{N}| < \frac{1}{N} \forall k} |\psi_{\mathbf{m}}(f(\mathbf{x}) - P_{\mathbf{m}}(\mathbf{x}))| \\
 &\leq \sum_{\mathbf{m}: |x_k - \frac{m_k}{N}| < \frac{1}{N} \forall k} |f(\mathbf{x}) - P_{\mathbf{m}}(\mathbf{x})| \tag{30} \\
 &\leq 2^d \max_{\mathbf{m}: |x_k - \frac{m_k}{N}| < \frac{1}{N} \forall k} |f(\mathbf{x}) - P_{\mathbf{m}}(\mathbf{x})| \\
 &\leq \frac{2^d d^n}{n!} \left(\frac{1}{N} \right)^n \max_{\mathbf{n}: |\mathbf{n}| \leq n} \text{ess sup}_{\mathbf{x} \in [0,1]^d} |D^{\mathbf{n}} f(\mathbf{x})| \\
 &\leq \frac{2^d d^n}{n!} \left(\frac{1}{N} \right)^n .
 \end{aligned}$$

Considering Equation (30), the first inequality simply uses a basic property of the absolute value function. The second one emerges from the fact that we now use a larger space for \mathbf{m} than before (as illustrated in Equation (29)). The third inequality uses the fact that $\sup_{\mathbf{x}} \psi_{\mathbf{m}} = 1$. The fourth inequality illustrates that there are at most 2^d terms in the summation and bounds by the maximum value of $|f(\mathbf{x}) - P_{\mathbf{m}}(\mathbf{x})|$. It is so because for a fixed value \mathbf{x} , at most 2^d combinations of \mathbf{m} exist such that $|x_k - \frac{m_k}{N}| < \frac{1}{N} \forall k$. The fifth one uses a standard bound for the Taylor remainder. The last one uses the fact that we only consider functions not in the Sobolev space $\mathcal{W}^{n,\infty}([0,1]^d)$ but in the unit ball $F_{n,d}$; it uses Equation (10).

The final manipulation of the first part of the proof is to choose wisely the value of N ; when choosing

$$\begin{aligned}
 \frac{\epsilon}{2} &= \frac{2^d d^n}{n!} \left(\frac{1}{N} \right)^n \\
 \Rightarrow N &= \left\lceil \left(\frac{n!}{2^{d+1} d^n} \frac{\epsilon}{2} \right)^{-1/n} \right\rceil ,
 \end{aligned}$$

it follows that

$$\|f - f_1\|_{\infty} \leq \frac{\epsilon}{2} .$$

Note that, because of how $F_{n,d}$ is defined (see Equation (10)), every coefficient of the polynomials $P_{\mathbf{m}}$ (that is, every term $\frac{D^{\mathbf{n}} f}{\mathbf{n}!} |_{\mathbf{x}=\frac{\mathbf{m}}{N}}$) is uniformly bounded by $1 \forall f \in F_{n,d}$. Therefore, expanding f_1 leads to the following:

$$f_1(\mathbf{x}) = \sum_{\mathbf{m} \in \{0,1,\dots,N\}^d} \sum_{\mathbf{n}: |\mathbf{n}| < n} a_{\mathbf{m},\mathbf{n}} \psi_{\mathbf{m}}(\mathbf{x}) \left(\mathbf{x} - \frac{\mathbf{m}}{N} \right)^{\mathbf{n}} , \quad |a_{\mathbf{m},\mathbf{n}}| \leq 1 . \tag{31}$$

Since every $a_{\mathbf{m},\mathbf{n}}$ is constant, f_1 is a linear combination of at most (as mentioned before) $d^n (N+1)^d$ terms $\psi_{\mathbf{m}}(\mathbf{x}) \left(\mathbf{x} - \frac{\mathbf{m}}{N} \right)^{\mathbf{n}}$. Each of these terms is a product of at most $d+n-1$ piece-wise linear univariate factors: d functions $h(3Nx_k - 3m_k)$ which compose $\psi_{\mathbf{m}}$ and at most $n-1$ linear expressions $x_k - \frac{m_k}{N}$ which compose $P_{\mathbf{m}}(\mathbf{x})$.

We now approximate f_1 with a sum of $d^n (N+1)^d$ binary activated feed-forward neural networks, each of them approximating a term $\psi_{\mathbf{m}}(\mathbf{x}) \left(\mathbf{x} - \frac{\mathbf{m}}{N} \right)^{\mathbf{n}}$ by applying recursively the function $\times'_{m,\delta}$ from Proposition 2.2, with an arbitrary parameter m and

maximum error rate δ to be chosen later, leading us to the following:

$$\tilde{f}_{\mathbf{m},n} = \times'_{m,\delta}(h(3Nx_1 - 3m_1), \times'_{m,\delta}(h(3Nx_2 - 3m_2), \dots, \times'_{m,\delta}(x_k - \frac{m_k}{N}, \dots) \dots)).$$

The value of m is then chosen so that when using $\times'_{m,\delta}(c, d)$, both $|c| < m$ and $|d| < m$ are respected. That is, we must find the largest number that could possibly be given as an argument to one of the functions \times' that appears in $\tilde{f}_{\mathbf{m},n}$. Since $\sup_{\mathbf{x}} = \sup_{\mathbf{x}} \psi_{\mathbf{m}} = 1 \forall \mathbf{m}$, the first application of a function \times' will be on arguments bounded by 1. On the second application, the first argument is bounded by 1 and the other, which is the result of the first application, bounded by $1 + \delta$, and so on. On the last application, the first argument is bounded by 1 while the other one is bounded by $1 + (d + n - 3)\delta$. Since $\delta < 1$, choosing $m = d + n - 2$ covers the worst case possible. Also, since there are $d + n - 2$ recursive calls, the depth of the network estimating $\tilde{f}_{\mathbf{m},n}$ is constant, but depends on d and n (depth $\propto d + n$).

Since $\tilde{f}_{\mathbf{m},n}$ contains $d + n - 2$ applications of \times' , whose error is bounded by δ , the maximum approximation error for $\left| \tilde{f}_{\mathbf{m},n} - \psi_{\mathbf{m}}(\mathbf{x}) \left(\mathbf{x} - \frac{\mathbf{m}}{N} \right)^{\mathbf{n}} \right|$ is given by $(d + n - 2)\delta$.

Now, all we need to do is define the full approximation of f by \tilde{f} and estimate the approximation error last two

$$\tilde{f} = \sum_{\mathbf{m} \in \{0,1,\dots,N\}^d} \sum_{\mathbf{n}: |\mathbf{n}| < n} a_{\mathbf{m},\mathbf{n}} \tilde{f}_{\mathbf{m},n} \quad (32)$$

$$\begin{aligned} |\tilde{f}(\mathbf{x}) - f_1(\mathbf{x})| &= \left| \sum_{\mathbf{m} \in \{0,1,\dots,N\}^d} \sum_{\mathbf{n}: |\mathbf{n}| < n} a_{\mathbf{m},\mathbf{n}} \left(\tilde{f}_{\mathbf{m},n} - \psi_{\mathbf{m}}(\mathbf{x}) \left(\mathbf{x} - \frac{\mathbf{m}}{N} \right)^{\mathbf{n}} \right) \right| \\ &= \left| \sum_{\mathbf{m}: \mathbf{x} \in \text{supp} \psi_{\mathbf{m}}} \sum_{\mathbf{n}: |\mathbf{n}| < n} a_{\mathbf{m},\mathbf{n}} \left(\tilde{f}_{\mathbf{m},n} - \psi_{\mathbf{m}}(\mathbf{x}) \left(\mathbf{x} - \frac{\mathbf{m}}{N} \right)^{\mathbf{n}} \right) \right| \\ &\leq \sum_{\mathbf{m}: \mathbf{x} \in \text{supp} \psi_{\mathbf{m}}} \sum_{\mathbf{n}: |\mathbf{n}| < n} \left| a_{\mathbf{m},\mathbf{n}} \left(\tilde{f}_{\mathbf{m},n} - \psi_{\mathbf{m}}(\mathbf{x}) \left(\mathbf{x} - \frac{\mathbf{m}}{N} \right)^{\mathbf{n}} \right) \right| \\ &\leq \sum_{\mathbf{m}: \mathbf{x} \in \text{supp} \psi_{\mathbf{m}}} \sum_{\mathbf{n}: |\mathbf{n}| < n} \left| \left(\tilde{f}_{\mathbf{m},n} - \psi_{\mathbf{m}}(\mathbf{x}) \left(\mathbf{x} - \frac{\mathbf{m}}{N} \right)^{\mathbf{n}} \right) \right| \\ &\leq 2^d \max_{\mathbf{m}: \mathbf{x} \in \text{supp} \psi_{\mathbf{m}}} \sum_{\mathbf{n}: |\mathbf{n}| < n} \left| \left(\tilde{f}_{\mathbf{m},n} - \psi_{\mathbf{m}}(\mathbf{x}) \left(\mathbf{x} - \frac{\mathbf{m}}{N} \right)^{\mathbf{n}} \right) \right| \\ &\leq 2^d d^n (d + n - 2) \delta. \end{aligned} \quad (33)$$

In Equation (33), the second equality illustrates that $\mathbf{x} \notin \text{supp} \psi_{\mathbf{m}} \Rightarrow \tilde{f}_{\mathbf{m},n} - \psi_{\mathbf{m}}(\mathbf{x}) \left(\mathbf{x} - \frac{\mathbf{m}}{N} \right)^{\mathbf{n}} = 0$, coming from (iv) of Proposition 2.2. The first inequality comes from a simple property of the absolute value function. The second one illustrates the fact that $|a_{\mathbf{m},\mathbf{n}}| \leq 1$, as pointed out in Equation (31). The third inequality consider that for any \mathbf{x} , there are at most $2^d \psi_{\mathbf{m}}(\mathbf{x})$ that are not equal to 0. The fourth one considers that every \mathbf{n} such that $|\mathbf{n}| < n$ leads to the worst case (there are d^n of them), where each one is equal to $(d + n)$.

Finally, if we choose

$$\delta = \frac{\epsilon}{2^{d+1} d^n (d + n - 2)},$$

for every $\times'_{m,\delta}$, then $\|\tilde{f} - f_1\|_{\infty} \leq \epsilon/2$ and (iii) is respected. By the triangular inequality, we have

$$\begin{aligned} \|\tilde{f} - f\|_{\infty} &\leq \|\tilde{f} - f_1\|_{\infty} + \|f_1 - f\|_{\infty} \\ &= \epsilon/2 + \epsilon/2 \\ &= \epsilon. \end{aligned}$$

As illustrated in Equation (32), \tilde{f} can be implemented by a weighted sum of $(N + 1)^d d^n$ parallel binary activated feed-forward neural networks; as shown in Proposition 2.2, each of these network has width in $O\left(\frac{1}{\delta}\right)$. Therefore, the total

network now has a width that is $(N + 1)^d d^n$ times bigger. Let's not forget that we chose $\delta = \frac{\epsilon}{2^{d+1} d^n (d+n)}$; the new width of the first layer is in $O\left(\frac{N^d d^n 2^{d+1} d^n (d+n)}{\epsilon}\right) = O\left(\frac{(2N)^d d^{2n} (d+n)}{\epsilon}\right)$. The upper bound of the depth will remain constant (a function of $d + n$), since doing an aggregation of weighted network will only add one layer.

Since we already fixed N , we can expand our width upper bound that way:

$$\begin{aligned} N^d \frac{d^{2n} (d+n)}{\epsilon} &= \left[\left(\frac{n! \epsilon}{2^d d^n 2} \right)^{-1/n} \right]^d \frac{d^{2n} (d+n)}{\epsilon} \\ &\approx \left(\frac{n! \epsilon}{2^d d^n 2} \right)^{-d/n} \frac{d^{2n} (d+n)}{\epsilon} \\ &= \left(\frac{n!}{2^{d+1} d^n} \right)^{-d/n} d^{2n} (d+n) \epsilon^{-(d/n+1)} \\ &= c \epsilon^{-(d/n+1)}, \end{aligned}$$

where c is a constant depending on fixed numbers; that is: n and d . Therefore, the width is in $O(c \epsilon^{-(d/n+1)})$, concluding the proof. \square

C.4. Proof of Theorem 1 (iii)

The following proof is inspired by the work of Yarotsky (2017). We will need the following technical lemma:

Lemma 1. *Let $a > 0$. Then: $x \geq 2a \log(a) \Rightarrow x \geq a \log(x)$. It follows that a necessary condition for the inequality $x < a \log(x)$ to hold is that $x < 2a \log(a)$.*

Theorem 1 (iii) *For $d, n \in \mathbb{N}^*$, there exists a binary activated network (i) which is capable of estimating any function from $F_{n,d}$ with maximum error ϵ ; (ii) for which the number of weights W is $\Omega(c \epsilon^{-d/n} \ln^{-1}(\epsilon^{-1}))$, where c is a constant depending on n and d .*

Proof. Let H be a class of Boolean functions on $[0,1]^d$. We are interested in the case where H is the family of functions obtained when applying a threshold function to a binary network with fixed architecture but variable weights. We will need both the concept of VC-dimension and the fact that, in our case:

$$\text{VCdim}(H) \in O(W \ln(W)), \quad (34)$$

where W is the number of weights in our network. Consider N , a positive integer to be chosen later. Now, select S , a set of N^d points $\mathbf{x}_1, \dots, \mathbf{x}_{N^d}$ in the hypercube $[0, 1]^d$ such that the distance between any two points from S is not less than $\frac{1}{N}$. Given any $\mathbf{y} = [y_1, \dots, y_{N^d}] \in \mathbb{R}^{N^d}$, we can construct a smooth function f satisfying $f(\mathbf{x}_m) = y_m \forall m$ by setting

$$f(\mathbf{x}) = \sum_{m=1}^{N^d} y_m \phi(N(\mathbf{x} - \mathbf{x}_m)),$$

with some C^∞ function $\phi : \mathbb{R}^d \rightarrow \mathbb{R}$ such that $\phi(\mathbf{0}) = 1$ and $\phi(\mathbf{x}) = 0$ if $|\mathbf{x}| > 1/2$. Now, we need to make sure that

$f \in F_{n,d}$:

$$\begin{aligned}
 \max_{\mathbf{x}} |D^n f(\mathbf{x})| &= \max_{\mathbf{x}} \left| D^n \left(\sum_{m=1}^{N^d} y_m \phi(N(\mathbf{x} - \mathbf{x}_m)) \right) \right| \\
 &= \max_{\mathbf{x}} \left| \sum_{m=1}^{N^d} y_m D^n \phi(N(\mathbf{x} - \mathbf{x}_m)) \right| \\
 &= \max_{\mathbf{x}} \left| \max_m y_m D^n \phi(N(\mathbf{x} - \mathbf{x}_m)) \right| \\
 &= \max_m |y_m| \max_{\mathbf{x}} |D^n \phi(N(\mathbf{x} - \mathbf{x}_m))| \\
 &= N^{|\mathbf{n}|} \max_m |y_m| \max_{\mathbf{x}} |D^n \phi(\mathbf{x} - \mathbf{x}_m)| \\
 &= N^{|\mathbf{n}|} \max_m |y_m| \max_{\mathbf{x}} |D^n \phi(\mathbf{x})| .
 \end{aligned}$$

The third equality comes from the fact that there are no points in S that are less than $\frac{1}{N}$ -far from each other; therefore, ϕ will yield 1 for only one term of the summation, which corresponds to the max of the function. Thus, the x maximizing $y_m D^n \phi(N(\mathbf{x} - \mathbf{x}_m))$ corresponds to the m maximizing y_m .

We got to make sure that $f \in F_{n,d}$: having $\max_m |y_m| \leq cN^{-n}$, where $c = (\max_{\mathbf{n}:|\mathbf{n}|\leq n} \max_x |D^n \phi(\mathbf{x})|)^{-1}$ is the first step.

We now set $\epsilon = \frac{cN^{-n}}{3}$. We suppose that there exists a binary activated feed-forward neural network that can approximate any function from $F_{n,d}$ with maximum error ϵ . We will denote by $\nu(\mathbf{x}, \mathbf{w})$ the output of the network for input \mathbf{x} and weights \mathbf{w} . Also, let $\mathbf{z} \in \{0, 1\}^{N^d}$ be any set of boolean N^d values. We set $y_m = z_m cN^{-n} \forall m \in \{1, 2, \dots, N^d\}$. Therefore, $f \in F_{n,d}$.

By assumption, there is then a vector of weights $\mathbf{w} = \mathbf{w}_{\mathbf{z}}$ such that for all m , we have $|\nu(\mathbf{x}_m, \mathbf{w}_{\mathbf{z}}) - y_m| \leq \epsilon$ and

$$\nu(\mathbf{x}_m, \mathbf{w}_{\mathbf{z}}) \begin{cases} \geq cN^{-n} - \epsilon > cN^{-n}/2, & z_m = 1 \\ \leq \epsilon < cN^{-n}/2, & z_m = 0, \end{cases}$$

so the thresholded network $\nu(\mathbf{x}_m, \mathbf{w}_{\mathbf{z}})_1 = 1_{\{\nu(\mathbf{x}_m, \mathbf{w}_{\mathbf{z}}) > cN^{-n}/2\}}$ outputs $z_m \forall m \in \{1, 2, \dots, N^d\}$. We thus conclude that z_m is shattered and that

$$VCdim(\nu_1) \geq N^d .$$

We previously defined $\epsilon = \frac{cN^{-n}}{3}$; by replacing N in the inequality, we obtain

$$VCdim(\nu_1) \geq \left(\frac{3\epsilon}{c} \right)^{-d/n} .$$

Using both Lemma 1 and Equation (34), since $W > 0$ and $\left(\frac{3\epsilon}{c}\right)^{-d/n} > 1$, we can bound W as follows:

$$\begin{aligned}
 W \ln(W) &\geq \left(\frac{3\epsilon}{c}\right)^{-d/n} \\
 \Rightarrow 2W \ln(W) &> \left(\frac{3\epsilon}{c}\right)^{-d/n} \\
 \Rightarrow W \ln\left(\left(\frac{3\epsilon}{c}\right)^{-d/n}\right) &> \left(\frac{3\epsilon}{c}\right)^{-d/n} \\
 \Rightarrow W &> \left(\frac{3\epsilon}{c}\right)^{-d/n} \ln^{-1}\left(\left(\frac{3\epsilon}{c}\right)^{-d/n}\right) \\
 \Rightarrow W &> \left(\frac{3\epsilon}{c}\right)^{-d/n} \left(-\frac{d}{n} \ln\left(\frac{3\epsilon}{c}\right)\right)^{-1} \\
 \Rightarrow W &> c^* \epsilon^{-d/n} \ln^{-1}(\epsilon^{-1})
 \end{aligned}$$

which concludes our proof. □

C.5. Proof of Proposition 3

Proposition 3. In Algorithm 2: $(c_t, d_t) = \operatorname{argmin}_{c,d} \sum_i \left(y_i^{(t)} - c \operatorname{sgn}(\mathbf{w}_t \cdot \mathbf{x}_i + b_t) - d\right)^2$.

Proof. Let's find the values of c and d in $\sum_i \left(y_i^{(t)} - c \operatorname{sgn}(\mathbf{w}_t \cdot \mathbf{x}_i + b_t) - d\right)^2$ for which the partial derivatives are zeros. We denote these values \hat{c} and \hat{d} respectively.

$$\begin{aligned}
 \frac{\partial}{\partial c} \sum_i \left(y_i^{(t)} - c \operatorname{sgn}(\mathbf{w}_t \cdot \mathbf{x}_i + b_t) - d\right)^2 &= -2 \sum_i \left(y_i^{(t)} - c \operatorname{sgn}(\mathbf{w}_t \cdot \mathbf{x}_i + b_t) - d\right) \operatorname{sgn}(\mathbf{w}_t \cdot \mathbf{x}_i + b_t) \\
 \Rightarrow 0 &= -2 \sum_i \left(y_i^{(t)} - \hat{c} \operatorname{sgn}(\mathbf{w}_t \cdot \mathbf{x}_i + b_t) - \hat{d}\right) \operatorname{sgn}(\mathbf{w}_t \cdot \mathbf{x}_i + b_t) \\
 \Rightarrow 0 &= \sum_i y_i^{(t)} \operatorname{sgn}(\mathbf{w}_t \cdot \mathbf{x}_i + b_t) - n\hat{c} - \sum_i \hat{d} \cdot \operatorname{sgn}(\mathbf{w}_t \cdot \mathbf{x}_i + b_t) \\
 \Rightarrow \hat{c} &= \frac{1}{n} \sum_i (y_i^{(t)} - \hat{d}) \cdot \operatorname{sgn}(\mathbf{w}_t \cdot \mathbf{x}_i + b_t)
 \end{aligned}$$

$$\begin{aligned}
 \frac{\partial}{\partial d} \sum_i \left(y_i^{(t)} - c \operatorname{sgn}(\mathbf{w}_t \cdot \mathbf{x}_i + b_t) - d\right)^2 &= -2 \sum_i \left(y_i^{(t)} - c \operatorname{sgn}(\mathbf{w}_t \cdot \mathbf{x}_i + b_t) - d\right) \\
 \Rightarrow 0 &= -2 \sum_i \left(y_i^{(t)} - \hat{c} \operatorname{sgn}(\mathbf{w}_t \cdot \mathbf{x}_i + b_t) - \hat{d}\right) \\
 \Rightarrow \hat{c} &= \frac{\sum_i y_i^{(t)} - n\hat{d}}{\sum_i \operatorname{sgn}(\mathbf{w}_t \cdot \mathbf{x}_i + b_t)}
 \end{aligned}$$

In order to lighten the notation, we write $\sum_{\pm 1}$ to denote $\sum_{i: \operatorname{sgn}(\mathbf{w}_t \cdot \mathbf{x}_i + b_t) = \pm 1}$.

$$\begin{aligned}
 & \frac{1}{n} \sum_i (y_i^{(t)} - \hat{d}) \text{sgn}(\mathbf{w}_t \cdot \mathbf{x}_i + b_t) = \frac{\sum_i y_i^{(t)} - n\hat{d}}{\sum_i \text{sgn}(\mathbf{w}_t \cdot \mathbf{x}_i + b_t)} \\
 \Rightarrow & \frac{(\sum_{+1} y_i^{(t)} - \sum_{-1} y_i^{(t)}) - \hat{d}(\sum_{+1} 1 - \sum_{-1} 1)}{\sum_{+1} 1 + \sum_{-1} 1} = \frac{(\sum_{+1} y_i^{(t)} + \sum_{-1} y_i^{(t)}) - \hat{d}(\sum_{+1} 1 + \sum_{-1} 1)}{\sum_{+1} 1 - \sum_{-1} 1} \\
 \Rightarrow & \hat{d}[(\sum_{+1} 1 + \sum_{-1} 1)^2 - (\sum_{+1} 1 - \sum_{-1} 1)^2] = (\sum_{+1} y_i^{(t)} + \sum_{-1} y_i^{(t)})(\sum_{+1} 1 + \sum_{-1} 1) \\
 & \quad - (\sum_{+1} y_i^{(t)} - \sum_{-1} y_i^{(t)})(\sum_{+1} 1 - \sum_{-1} 1) \\
 \Rightarrow & 4\hat{d} \sum_{+1} 1 \sum_{-1} 1 = 2 \sum_{+1} y_i^{(t)} \sum_{-1} 1 + 2 \sum_{-1} y_i^{(t)} \sum_{+1} 1 \\
 \Rightarrow & \hat{d} = \frac{1}{2} \left(\frac{\sum_{+1} y_i^{(t)}}{\sum_{+1} 1} + \frac{\sum_{-1} y_i^{(t)}}{\sum_{-1} 1} \right)
 \end{aligned}$$

$$\begin{aligned}
 \hat{c} &= \frac{\sum_i y_i^{(t)} - n\hat{d}}{\sum_i \text{sgn}(\mathbf{w}_t \cdot \mathbf{x}_i + b_t)} \\
 \Rightarrow \hat{c} &= \frac{\sum_{+1} y_i^{(t)} + \sum_{-1} y_i^{(t)}}{\sum_{+1} 1 - \sum_{-1} 1} - \hat{d} \frac{\sum_{+1} 1 + \sum_{-1} 1}{\sum_{+1} 1 - \sum_{-1} 1} \\
 \Rightarrow \hat{c} &= \frac{\sum_{+1} y_i^{(t)} + \sum_{-1} y_i^{(t)}}{\sum_{+1} 1 - \sum_{-1} 1} - \frac{1}{2} \left(\frac{\sum_{+1} y_i^{(t)}}{\sum_{+1} 1} + \frac{\sum_{-1} y_i^{(t)}}{\sum_{-1} 1} \right) \frac{\sum_{+1} 1 + \sum_{-1} 1}{\sum_{+1} 1 - \sum_{-1} 1} \\
 \Rightarrow \hat{c}(\sum_{+1} 1 - \sum_{-1} 1) &= \sum_{+1} y_i^{(t)} + \sum_{-1} y_i^{(t)} - \frac{1}{2} \frac{\sum_{+1} y_i^{(t)} \sum_{-1} 1 + \sum_{-1} y_i^{(t)} \sum_{+1} 1}{\sum_{+1} 1 \sum_{-1} 1} (\sum_{+1} 1 + \sum_{-1} 1) \\
 \Rightarrow \hat{c}(\sum_{+1} 1 - \sum_{-1} 1) &= \frac{1}{2} \sum_{+1} y_i^{(t)} + \frac{1}{2} \sum_{-1} y_i^{(t)} - \frac{1}{2} \frac{\sum_{+1} y_i^{(t)} \sum_{-1} 1}{\sum_{+1} 1} - \frac{1}{2} \frac{\sum_{-1} y_i^{(t)} \sum_{+1} 1}{\sum_{-1} 1} \\
 \Rightarrow \hat{c}(\sum_{+1} 1 - \sum_{-1} 1) &= \frac{1}{2} \frac{\sum_{+1} y_i^{(t)} (\sum_{+1} 1 - \sum_{-1} 1)}{\sum_{+1} 1} - \frac{1}{2} \frac{\sum_{-1} y_i^{(t)} (\sum_{+1} 1 - \sum_{-1} 1)}{\sum_{-1} 1} \\
 \Rightarrow \hat{c} &= \frac{1}{2} \left(\frac{\sum_{+1} y_i^{(t)}}{\sum_{+1} 1} - \frac{\sum_{-1} y_i^{(t)}}{\sum_{-1} 1} \right)
 \end{aligned}$$

□

C.6. Proof of Proposition 4

Proposition 4. *In Algorithm 2, we have*

$$Q(BGN_{t-1}, S) - Q(BGN_t, S) = (c_t + d_t)(c_t - d_t) > 0, \forall t \in \mathbb{N} \setminus \{0, 1\}.$$

Proof. Let's use the shortcut notation $\sum_{\pm 1}$ to denote $\sum_{i: \text{sgn}(\mathbf{w}_t \cdot \mathbf{x}_i + b_t) = \pm 1}$.

$$\begin{aligned} d_t - c_t &= \frac{1}{2} \left(\frac{\sum_{+1} y_i}{\sum_{+1} 1} + \frac{\sum_{-1} y_i}{\sum_{-1} 1} \right) - \frac{1}{2} \left(\frac{\sum_{+1} y_i}{\sum_{+1} 1} - \frac{\sum_{-1} y_i}{\sum_{-1} 1} \right) \\ &= \frac{\sum_{-1} y_i}{\sum_{-1} 1}, \\ d_t + c_t &= \frac{1}{2} \left(\frac{\sum_{+1} y_i}{\sum_{+1} 1} + \frac{\sum_{-1} y_i}{\sum_{-1} 1} \right) + \frac{1}{2} \left(\frac{\sum_{+1} y_i}{\sum_{+1} 1} - \frac{\sum_{-1} y_i}{\sum_{-1} 1} \right) \\ &= \frac{\sum_{+1} y_i}{\sum_{+1} 1}. \end{aligned}$$

We first show that $Q(BGN_{t-1}, S) - Q(BGN_t, S) > 0, \forall t \in \mathbb{N} \setminus \{0, 1\}$.

$$\begin{aligned} &Q(BGN_{t-1}, S) - Q(BGN_t, S) \\ &= \frac{1}{m} \sum_{i=1}^m (y_i - BGN_{t-1}(\mathbf{x}_i))^2 - \frac{1}{m} \sum_{i=1}^m (y_i - BGN_t(\mathbf{x}_i))^2 \\ &= \frac{1}{m} \sum_{i=1}^m \left(y_i^{(t)} \right)^2 - \frac{1}{m} \sum_{i=1}^m \left(y_i^{(t)} - c_t h_t(\mathbf{x}_i) - d_t \right)^2 \\ &= \frac{1}{m} \sum_{i=1}^m \left(y_i^{(t)} \right)^2 - \frac{1}{m} \sum_{i=1}^m \left(\left(y_i^{(t)} \right)^2 - 2y_i^{(t)}(c_t h_t(\mathbf{x}_i) + d_t) + (c_t h_t(\mathbf{x}_i) + d_t)^2 \right) \\ &= \frac{1}{m} \sum_{i=1}^m \left(2y_i^{(t)}(c_t h_t(\mathbf{x}_i) + d_t) - (c_t h_t(\mathbf{x}_i) + d_t)^2 \right) \\ &= c_t \frac{2}{m} \sum_{i=1}^m y_i^{(t)} h_t(\mathbf{x}_i) + d_t \frac{2}{m} \sum_{i=1}^m y_i^{(t)} - \frac{1}{m} \sum_{i=1}^m \underbrace{c_t^2 h_t^2(\mathbf{x}_i)}_{=1 \forall \mathbf{x}} - \frac{1}{m} \sum_{i=1}^m d_t^2 - c_t d_t \frac{2}{m} \sum_{i=1}^m h_t(\mathbf{x}_i) \\ &= \frac{1}{m} \left[\left(\frac{\sum_{+1} y_i^{(t)}}{\sum_{+1} 1} - \frac{\sum_{-1} y_i^{(t)}}{\sum_{-1} 1} \right) \left(\sum_{+1} y_i - \sum_{-1} y_i \right) + \left(\frac{\sum_{+1} y_i^{(t)}}{\sum_{+1} 1} + \frac{\sum_{-1} y_i^{(t)}}{\sum_{-1} 1} \right) \left(\sum_{+1} y_i + \sum_{-1} y_i \right) \right. \\ &\quad - \frac{1}{4} \left(\frac{\sum_{+1} y_i^{(t)}}{\sum_{+1} 1} - \frac{\sum_{-1} y_i^{(t)}}{\sum_{-1} 1} \right)^2 \left(\sum_{+1} 1 + \sum_{-1} 1 \right) - \frac{1}{4} \left(\frac{\sum_{+1} y_i^{(t)}}{\sum_{+1} 1} + \frac{\sum_{-1} y_i^{(t)}}{\sum_{-1} 1} \right)^2 \left(\sum_{+1} 1 + \sum_{-1} 1 \right) \\ &\quad \left. - \frac{1}{2} \left(\frac{\sum_{+1} y_i^{(t)}}{\sum_{+1} 1} - \frac{\sum_{-1} y_i^{(t)}}{\sum_{-1} 1} \right) \left(\frac{\sum_{+1} y_i^{(t)}}{\sum_{+1} 1} + \frac{\sum_{-1} y_i^{(t)}}{\sum_{-1} 1} \right) \left(\sum_{+1} 1 - \sum_{-1} 1 \right) \right] \\ &= \frac{1}{m} \left[2 \frac{\left(\sum_{+1} y_i^{(t)} \right)^2}{\sum_{+1} 1} + 2 \frac{\left(\sum_{-1} y_i^{(t)} \right)^2}{\sum_{-1} 1} - \frac{1}{2} \left(\frac{\left(\sum_{+1} y_i^{(t)} \right)^2}{\left(\sum_{+1} 1 \right)^2} + \frac{\left(\sum_{-1} y_i^{(t)} \right)^2}{\left(\sum_{-1} 1 \right)^2} \right) \left(\sum_{+1} 1 + \sum_{-1} 1 \right) \right. \\ &\quad \left. - \frac{1}{2} \left(\frac{\left(\sum_{+1} y_i^{(t)} \right)^2}{\left(\sum_{+1} 1 \right)^2} - \frac{\left(\sum_{-1} y_i^{(t)} \right)^2}{\left(\sum_{-1} 1 \right)^2} \right) \left(\sum_{+1} 1 - \sum_{-1} 1 \right) \right] \\ &= \frac{1}{m} \left[2 \frac{\left(\sum_{+1} y_i^{(t)} \right)^2}{\sum_{+1} 1} + 2 \frac{\left(\sum_{-1} y_i^{(t)} \right)^2}{\sum_{-1} 1} - \frac{\left(\sum_{+1} y_i^{(t)} \right)^2}{\sum_{+1} 1} - \frac{\left(\sum_{-1} y_i^{(t)} \right)^2}{\sum_{-1} 1} \right] \\ &= \frac{1}{m} \left[\frac{\left(\sum_{+1} y_i^{(t)} \right)^2}{\sum_{+1} 1} + \frac{\left(\sum_{-1} y_i^{(t)} \right)^2}{\sum_{-1} 1} \right] > 0 \end{aligned}$$

Since we have that

$$\left(\sum_{+1} y_i^{(t)}\right)^2 \left(\sum_{-1} 1\right) + \left(\sum_{-1} y_i^{(t)}\right)^2 \left(\sum_{+1} 1\right) + \left(\sum_{+1} y_i^{(t)}\right) \left(\sum_{-1} y_i^{(t)}\right) \left(\sum_{+1} 1 + \sum_{-1} 1\right) = 0,$$

then

$$\begin{aligned} Q(BGN_{t-1}, S) - Q(BGN_t, S) &= \frac{1}{m} \left[\frac{\left(\sum_{+1} y_i^{(t)}\right)^2}{\sum_{+1} 1} + \frac{\left(\sum_{-1} y_i^{(t)}\right)^2}{\sum_{-1} 1} \right] \\ &= \frac{1}{m} \left[\frac{\left(\sum_{+1} y_i^{(t)}\right)^2 (\sum_{-1} 1) + \left(\sum_{-1} y_i^{(t)}\right)^2 (\sum_{+1} 1)}{(\sum_{+1} 1) (\sum_{-1} 1)} \right] \\ &= -\frac{1}{m} \left[\frac{m \left(\sum_{+1} y_i^{(t)}\right) \left(\sum_{-1} y_i^{(t)}\right)}{(\sum_{+1} 1) (\sum_{-1} 1)} \right] \\ &= -\left(\frac{\sum_{+1} y_i^{(t)}}{\sum_{+1} 1}\right) \left(\frac{\sum_{-1} y_i^{(t)}}{\sum_{-1} 1}\right) \\ &= -(d_t + c_t)(d_t - c_t) \\ &= (c_t + d_t)(c_t - d_t) \end{aligned}$$

□